Catalysis Science & Technology

Accepted Manuscript

ROYAL SOCIETY OF CHEMISTRY

www.rsc.org/catalysis

Journal Name

RSCPublishing

REVIEW

Insights into mesoporous metal phosphonate hybrid materials for catalysis

Cite this: DOI: 10.1039/x0xx00000x

Yun-Pei Zhu,[a] Tie-Zhen Ren[b] and Zhong-Yong Yuan*,[a]

Received 00th January 2012,
Accepted 00th January 2012

DOI: 10.1039/x0xx00000x

www.rsc.org/

Catalysis is crucial for sustainable process management. The discovery of mesoporous metal phosphonate hybrid materials has opened great opportunities for new applications in catalysis, thanks to the homogeneous composition, the combined merits of inorganic units and organic groups, and the considerable porosity. In this review, we present the fundamentals for designing and optimizing hybrid mesostructures and the recent progress to the fields of metal phosphonate-based catalytic reactions. The catalytic reactions are on the basis of three categories, *i.e.*, metal sites, organophosphonate moieties, and potential precursors for active metal phosphates. Each section highlights the recent advances and the corresponding reactions are discussed in detail. Direct functionalization of the mesopore surfaces of the hybrids, such as sulfonation and supporting, features an elegant way to bridge the gap between heterogeneous and homogeneous catalysis. Moreover, remarks on the challenges and perspectives are presented for further exploration of mesoporous metal phosphonate hybrid heterogeneous catalysts.

1. Introduction

Catalysis is of tremendous significance in the areas of industrial production, scientific research, and even human daily life. A number of efforts have been made in the past for rational design of catalysts so as to achieve desirable catalytic activity and selectivity, though recovery of the catalyst was not really a serious concern. Classical homogeneous catalytic systems have been proven to be considerably efficient since they are well defined on a molecular level and readily soluble in the reaction medium, ensuring sufficient contact between the catalysts and the reactants,[1-5] but removing them from the reaction mixture to avoid contamination of the target products needs expensive and tedious purification procedures. Furthermore, in spite of the intrinsic superiorities, the corresponding components usually are consisted of high–priced noble metal and/or ligands, making the homogeneous catalysts find difficulties in wide application in the industrial processes.[6,7] Accordingly, the recovery and reuse of catalysts become an important factor that should be taken into consideration, because of stringent ecological and economical demands from the viewpoints of green chemistry and sustainable environment and energy. To realize the advantages of homogeneous and heterogeneous catalysis synchronously, heterogenization of homogeneous catalysts and exploration of alternative heterogeneous catalysts represent feasible solutions.[8,9]

The intentional development of structured heterogeneous catalysts, underpinned be the knowledge of basic structural-function relationships, has been the motivation to deliver enhanced catalysis. Solid catalysts of inorganic frameworks with favourable mechanical rigidity and thermal stability including silicate– and phosphate–based molecular sieves,[10-12] mesoporous carbons,[13,14] carbon nanostructures,[15-17] and metal oxides or sulfides[18-21] have exhibited practical applicability. For instance, crystalline microporous zeolites have been testified to be extremely successful as catalysts in oil refining, petrochemistry, and organic synthesis for the production of fine and special chemicals.[22,23] However, the dimensions and accessibility of the pores are restrained to the subnanometer scale; on the other side, extra–large pore or supermicroporous materials with inorganic framework compositions were synthesized,[24] but the lack of flexibility of the inorganic networks and the inertness towards further functionalization have prompted researchers to explore organic–inorganic hybrid materials.

The use of hybrid materials comprised of intimately cross-linked organic and inorganic building units at the molecular scale aims to integrate the superiorities of both components within the backbones, holding the promise for the formation of materials with mechanical and structural stability of inorganic materials, and with the flexibility and functionality characteristic of organic compounds.[25] The choice of metal centers and organic linkers can dedicate the framework topology and affect the overall physicochemical functionality of the hybrid skeleton, which in turn can influence the performances of the hybrid materials for chemical, electrochemical, and biochemical activities, as well as on magnetic, electronic, and optical properties, and even a combination of them.[26-29] These traits uncover a way to the creation of materials bearing diverse localized active groups or sites, leading to the generation of marvellous multifunctional hybrid materials with unique and unknown properties. Besides, the modulation of interesting properties can be favoured by the interface features present in the hybrids, owing to the molecular interaction existing between inorganic and organic phases, which is of paramount significance for catalytic processes in terms of transfer.

Heterogeneous catalysis dependent on the organic–inorganic hybrids is quite intriguing as compared with the pure inorganic catalysts. For the sake of catalytic reaction processes, adjustable functions can be obtained through judiciously selecting the organic bridging groups and inorganic precursors due to the well–aligned sequences of framework compositions.[30,31] Moreover, it is probable to mimic the basic principles of natural enzymatic catalysis, wherein weak interaction such as electrostatic interaction and hydrogen bonding between the functional groups at fixed distances influence the reactivity of the catalysts.[32,33] Mesoporous organosilicas and organo-functionalized mesoporous silicas have been dedicated as efficient heterogeneous catalysts through the introduction of metal sites and organometallic ligands and post-modification. However, their further potency towards practical applications are prohibited by the high price of the organosilicane reagents and the unfavourable synthesis strategy that leads to the inferior distribution of catalytic sites and even sacrifice of porosity, which may be due to the incompatibility between the metal sites and organosilica networks. Pyridine, sulfonate, and carboxylate based organic scaffolds have been used to construct organic–inorganic hybrid due to the strong coordinative interaction with the metallic centers.[34-37] In comparison with these organic linkage counterparts, metal phosphonates exhibit much higher thermal and chemical stability due to the corresponding tetrahedral nature and the strong affinity of organophosphonic ligating linkers to metal ions, making them promising in the fields of catalysis, energy conversion, adsorption, biotechnology and so forth.[25,34,35,38,39]

The different reactivity of phosphonic coupling molecules leads to structural diversity and physicochemical peculiarities of the resultant hybrid materials. At this juncture, metal phosphonates with especially high specific surface areas, controllable pore size, and large pore volume can contribute towards an enhanced performances as the homogeneous distribution of active sites on the hybrid pore walls. Several tactics have been employed to create porosity in metal phosphonates. Adjustment of phosphonate linkers, generally involving inserting non–pillaring phosphonic/phosphoric groups,[42] extending the microscopic dimension and geometry of polyphosphonic bridging molecules,[43-45] and attaching a secondary functional group,[46] provide reasonable methods. Recently, template–free approaches including nanocrystal self–assembly and microemulsion based on that the preformed metal phosphonate nanoclusters or nanoparticles performed as building units are taken to prepare mesoporous metal phosphonate hybrid materials, wherein weak interactions among the building blocks, including atoms, molecules, and related secondary units are required to direct the assembly process.[34,35,47,48] To synthesize mesoporous metal phosphonates with much more controllable mesopososity, surfactant–assisted sol–gel methodology has been thoroughly developed for the design of periodic mesoporous materials, in which the surfactant micelle scaffold acts as a lyotropic liquid crystalline phase, and subsequently the oligomers from the condensation of inorganic/organic precursors condense and polymerize around the arranged micelles, leading to the assembly of an ordered mesostructure.[41] Accordingly, a series of periodic mesoporous metal phosphonate materials with tuneable pore size and mesophases can be successfully prepared by simply varying the surfactant types and controlling the synthesis conditions.[49-54] One can thus choose the right strategy for the synthesis of mesoporous metal phosphonates, which mainly depend on the ultimate usage.

A number of reviews have summarized the synthesis, characterization, and emerging applications of metal

Yun-Pei Zhu

Yun-Pei Zhu received his BSc degree in 2011 at Henan Polytechnic University. He is currently a PhD candidate under the supervision of Prof. Zhong-Yong Yuan at Nankai University. He was awarded the Top-Ten Youth of Nankai University, and a winner of the National Scholarship in 2014. His current research relates to the rational design and practical applications of porous organic–inorganic hybrid materials and nanostructured carbons.

Tie-Zhen Ren

Tie-Zhen Ren obtained her PhD degree from the University of Namur, Belgium in 2005. After two-year postdoctoral research at Stockholm University, Sweden, she joined the faculty of the Hebei University of Technology in 2007, where she is currently Professor in Chemical Technology. Her group's research areas include nanoporous photoelectrochemical materials and metal-organic frameworks. She is co-author of 90 ISI publications.

Zhong-Yong Yuan

Zhong-Yong Yuan received his PhD degree from Nankai University in 1999. After his postdoctoral research at the Institute of Physics, Chinese Academy of Sciences, he joined the Laboratory of Inorganic Materials Chemistry at the University of Namur, Belgium in 2001. In 2005, he was appointed Professor in Nankai University. In 2006, he was awarded the "Program for New Century Excellent Talents in University" by the Ministry of Education. His research interests are mainly focused on the self-assembly of hierarchically nanoporous and nanostructured materials for energy and environmental applications. He is coauthor of 200 ISI publications, 1 book and 4 book chapters, and 11 patents.

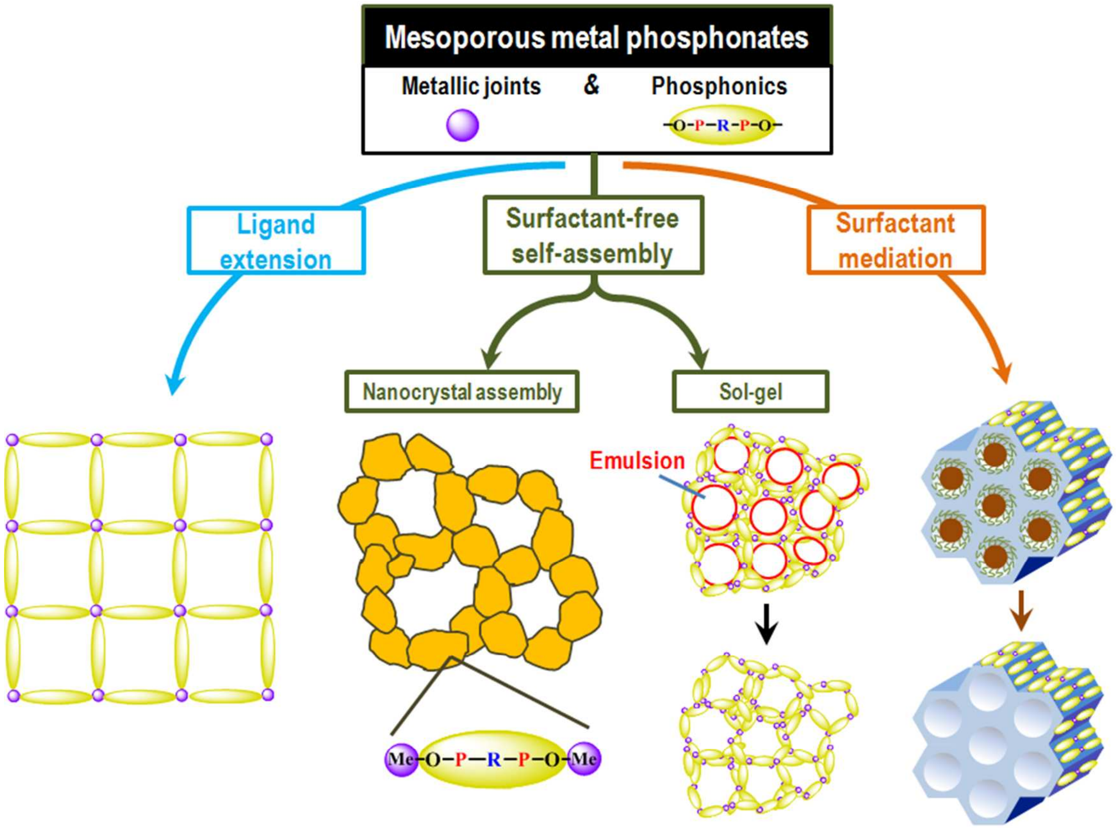

Fig. 1 Schematic illustration of three typical methods for synthesizing mesoporous metal phosphonates.

phosphonates.[25,31,35,55] However, only limited investigations of metal phosphonates have been carried out in heterogeneous catalysis as compared with the achievement in adsorption and separation. Brief introduction concerning metal phosphonates in the area of catalysis have been presented previously,[34,35,38] but the elaborated discussion and comparison of the origin of catalytic activities, reaction mechanisms and function adjustment are still scarcely considered. On the consideration of peculiarities for mesoporous organic–inorganic hybrids of metal phosphonates and their recent achievements, this review provides comprehensive understanding of this kind of heterogeneous hybrid catalysts in three aspects, *i.e.*, metal site based catalysis, catalytic activities from the phosphonate groups, and the extended functionalities via post–modification that is mainly dependent on the homogeneously immobilized organophosphonate linkages, and potential for the synthesized metal phosphates. Here it should be noteworthy that the cooperative effect from both sides is indispensable for an actual reaction process. To facilitate the reading of this review, the general synthetic approaches explored to date for the designed construction of mesoporous metal phosphonate hybrid materials are briefly described in the second part of this article. The catalytic reactions involving mesoporous metal phosphonates are summarized and discussed in detail, while the final conclusion part remarks on the future challenges and perspectives. It is suggested that the promising mesoporous heterogeneous metal phosphonate catalysts could receive deep attention from materials scientists and chemists who are devoting themselves to designing novel systems for burgeoning catalysis.

2. Strategies to introduce mesoporosity

Judicious design of well–defined mesoporous materials with large surface areas, controllable composition of pore walls and the intentional tailoring of mesopore architectures affords potential and advances in a diversity of fields including catalysis, adsorption, storage, separation, electronics, and bio-applications. The porous and structural capacities at the nano– or mesoscale can cater to the demands of the applications emerging for large molecules. Consequently, scientific researchers across the world have been interested in exploring and exploiting of mesoporous materials. As to the classical mesoporous siliceous materials and carbons, the introduction of well-defined mesostructures seems easy since the key factors are widely known, such as surfactant types and their concentrations, system temperature, media, precursors, and so on. Samples synthesized even under similar conditions actually present distinctively distinguishing properties. For mesoporous metal phosphonate hybrid materials, the synthesis is somewhat different from the inorganic porous materials, but their synthesis processes are still comparable. The use of organophosphonic bridging molecules makes the apparent strategies and the resultant mesoporosity much more abundant. The complicated synthesis systems vary with the change of microenvironment, and a complex combination of simple factors will offer great opportunities in creating different mesoporous architectures. Broadly speaking, extending the dimension of phosphonate groups, template–free self–assembly and surfactant–mediated strategies represents the three major

Table 1. Summary of synthetic parameters and physicochemical properties of mesoporous metal phosphonate hybrid materials.

Synthesis strategy		Metallic precursor	Phosphor source[a]	Surface area/ $m^2 g^{-1}$	Pore size/ nm	Pore volume/ $cm^3 g^{-1}$	Surfactant	Mesophase	Organic additive[b]	Crystalline phase	Ref.
Ligand extension		$DyCl_3$	PPMP	81	0.4	0.029	–	–	–	–	59
		$Ti(O)(i\text{-}Pr)_4$	TPPhA	557	3.8	0.42	–	–	–	Amorphous	44
		$V(O)(i\text{-}Pr)_4$	TPPhA	118	3.8-3.9	–	–	–	–	–	45
		$Ti(O)(n\text{-}Bu)_4$	BHMTPMPA	307	2.7	0.21	–	–	–	Amorphous	131
Template-free self-assembly	Nanocrystal self-assembly	$NiCl_2$	EDTMP, H_3PO_4	267	5.3	0.191	–	–	–	Nickel phosphate	118
		$Ti(O)(i\text{-}PrO)_4$	BTPA	255	1.4-4.8	0.464	–		–	Triclinic phase	97
		$SnCl_4$	BTPA	380	1.3, 3.5	0.155	–	–	–	Hexagonal phase	108
		$MoCl_5$	BTPA	183	1.6, 2.7	0.148	–	–	Ethanol	Orthorhombic phase	109
		$FeCl_3$	BTPA	556	1.1, 2.1	0.293	–	–	–	Triclinic phase	113
		$FeCl_3$	HDTMP	154	4.5	0.35	–	–	–	Tetragonal phase	110
		$SnCl_4$	PA	347	1.5, 2.5	–	–	–	–	–	116
		$NiCl_2$	HDTMP	241	1.3, –	0.29	–	–	–	Tetragonall phase	119
		$SnCl_4$	PDP, n=4	338	1.2-6.8	5.4	–	–	–	Tetragonal phase	124
		$ZnCl_2$	PDP, n=8	105	5.8	0.39	–	–	–	Orthorhombic phase	134
	Sol-gel	$Ti(O)(n\text{-}Bu)_4$	EDTMP	257	2.0	0.263	–	–	Ethanol	Anatase-phosphonate	48
		$Ti(O)(n\text{-}Bu)_4$	EDTMP	86	2.5–10	0.074	–	–	Ethanol	Anatase-phosphonate	93
		$MnCl_2$	EDTMP	66	4-30	0.095	–	–	–	Amorphous	123
		$Ti(O)(n\text{-}Bu)_4$	DTPMPA	128	3.6	0.19	–	–	Ethanol	Anatase-phosphonate	133
		$Ti(O)(n\text{-}Bu)_4$	DTPMPA	269	5.1	0.22	–	–	–	Amorphous	134
		$Al(O)(s\text{-}Bu)_3$	ATMP	77	4.3	0.38	–	–	–	Amorphous	150
Surfactant-mediated synthesis		$CeCl_3$	EDTMP	455	3-30	0.93	$C_{16}TABr$	Worm-like mesopore	–	Amorphous	26
		$TiCl_4$	AST	705	2-3	0.53	Brij 56	Worm-like mesopore	Ionic liquid	Anatase-phosphonate	27
		$TiCl_4$	EDTMP	522	1.4, 7.2	0.54	F127	hexagonal	Ethanol	Crystalline titanium phosphonate	39
		$AlCl_3$	PDP, n=1	579	3.3	0.53	Brij 56	Hexagonal	Ethanol	–	51
		$AlCl_3$	PDP, n=1	185	9.2	0.47	P123	Hexagonal	Ethanol	–	51
		$Al(O)(i\text{-}Pr)_3$	PDP, n=1	738	1.8	0.32	$C_{18}TACl$	Hexagonal	TMAH	–	52
		$AlCl_3$	PDP, n=1	738	1.9	0.37	$C_{18}TACl$	Hexagonal	TMAH	–	53
		$AlCl_3$	PDP, n=2	732	1.9	0.38	$C_{16}TACl$	Hexagonal	Ethanol	–	53
		$AlCl_3$	PDP, n=3	71	–	0.04	$C_{16}TACl$	–	Ethanol	–	53
		$TiCl_4$	HEDP	1052	2.6	0.58	$C_{16}TABr$	Cubic	Ethanol	Amprphous	54
		$Al(O)(s\text{-}Bu)_3$	PDP, n=2	713	3.3	0.85	$C_{16}TABr$	Hexagonal	TEAH	–	76
		$Al(O)(s\text{-}Bu)_3$	PDP, n=1	655	3.4	0.86	$C_{16}TABr$	Hexagonal	TEAH	–	77
		$Al(O)(s\text{-}Bu)_3$	PDP, n=2	674	3.3	0.63	$C_{16}TABr$	Hexagonal	TEAH	–	77
		$Al(O)(i\text{-}Pr)_3$	PDP, n=1, 2	–	–	–	$C_{16}TACl$	Lamellar	–	Crystalline aluminum phosphonate	80
		$TiCl_4$	EDTMP	1066	2.8	0.83	Brig 56	Hexagonal	Ethanol	Amorphous	94
		$TiCl_4$	AST	540	2.4	0.43	Brig 56	Hexagonal	Ethanol	Amorphous	141
		$TiCl_4$	HEDP	1037	2.4	0.57	Brig 56	Hexagonal	Ethanol	Amorphous	146
		$ZrOCl_2$	HEDP	702	3.6	0.86	$C_{16}TABr$	Worm-like mesopore	Ethanol	Amorphous	132
		$Ti(O)(n\text{-}Bu)_4$	ATMP	307	2-13	0.38	F127	Worm-like mesopore	Ethanol	Anatase-phosphonate	167
		$TiCl_4$	EDTMP	606	2.2	0.44	Brij 56	Hexagonal	Ethanol	Amorphous	170

[a] PPMP = (S)-N-(phosphonomethyl)proline, BHMTPMPA = bis(hexamethylene triamine penta (methylene phosphonicacid)) BTPA = benzene-1,3,5-triphosphonic acid, HDTMP = hexamethylenediamine-N,N,N',N'-tetrakis-(methylphosphonic acid), PA = phytic acid, PDP = propylene diphosphonic acid, DTPMPA = diethylene triamine penta(methylene phosphonic acid), AST = alendronate sodium trihydrate. [b] TMAH = tetramethylammonium hydroxide.

routes to prepare mesoporous metal phosphonate materials, which have been summarized in **Fig. 1**. Also, the syntheses, textures and physicochemical properties of mesoporous metal phosphonates are presented in **Table 1**.

2.1 Extending the dimension of phosphonate groups

The adjustable properties of the original phosphonic linkages make the synthesis of mesoporous metal phosphonates different from that of mesoporous pure inorganic materials. It is pertinent to mention the layered structures of metal phosphonates, in which aryl- or alkylphosphonate molecules are coordinated to metal oxide layers with the aryl or alkyl functional groups tightly situated in the interlamellar spaces.[56,57] The phosphonate pillars are too crowded to leave sufficient free space in the interlayer regions, so no or poor porosity is expected. As "dilution agents", some small alkyl or aryl biphosphonic acids were inserted among the phosphonate pillaring groups to induce an interlayer porosity.[43] But the resultant pore size is usually limited in the microporous range. Grafting secondary functional groups onto the pillared biphosphonic acids could lead to an increase in the surface area of the resulting hybrid materials, which was attributable to the formation of intralayer voids.[46,58] This method was used to overcome the "close-pillar disposition". This increase in porosity allowed the metal centers and phosphonate functionalities of the metal phosphonate to be accessible to the adsorbed molecules, which could be particularly valuable for catalysis. Amino acid derived phosphonates could be used to form mesoporous architectures of lanthanide phosphonate solids.[59] The chiral (*S*)-*N*-(phosphonomethyl)proline was reacted with several lanthanides to form isostructural solids with 1D tubular channels of about 4 nm in diameter. A large and multidimensional polyphosphonic bridging molecule, 1,3,5,7-tetrakis(4-phenylphosphonic acid)-adamantane (TPPA), would disfavour the formation of the layered motif, thus resulting in an open framework.[44,45] Through an non–hydrolytic condensation reaction, mesoporous titanium[44] and vanadium[45] phosphonates could be constructed using the corresponding metal alkoxide precursors. N_2 sorption analysis confirmed the high surface area and mesopores with size centered around 3.8 nm for the mesoporous titanium phosphonate hybrid.[44]

Ligand extension is a direction way to improve the porosity, though the most multi–dimensional structures of phosphonates, which are not commercially available, complicate their synthetic technologies. Meanwhile, bridging linker expansion tends to reduce the surface areas and pore sizes because of the consequent interpenetrated structures, and dramatically reduces the stability of the hybrid frameworks.[60,61] The ordered nanostructures or pores could only be retained for small mesopore sizes or constricted cages.

2.2 Template–free self–assembly

Self–assembly in the absence of any surfactants or templates typically initiates the weak interactions among the precursor molecules or the preformed primary phosphonates building blocks,[62] followed by the ordered attachment to generate mesoporous frameworks. Zirconium phosphite-phosphonates with high surface area and large pore volume were obtained via simply changing the ratios and the concentrations of the reagents.[63] The formation of interparticle mesoporosity was attributable to the edge–edge interactions between rigid packets of a few pillared α-layers giving rise to stable aggregates with a house of cards structure. The preformed nickel phosphate nanoparticles could mediate the self–assembly process to conduct the formation of mesoporous nickel phosphate/phosphonate hybrid microspheres (**Fig. 2a** and **b**).[64] The accessibility of this method lies in the fact of the water insolubility of nickel phosphate and the nature of phosphonate claw molecules containing pyridinic nitrogen, which could facilitate hydrogen bonding interactions between the phosphate nanoparticles and the slowly formed phosphonates.

The strong coordination ability of phosphonic groups to metal units promotes the deposition of dense metal phosphonates through regular methodologies. Aerogel approach involving sub/supercritical conditions could efficiently prohibit the metal ions and phosphonic linkers to orderly assemble into extended hybrid skeletons, due to the inhibited and mismatched growth and the following gelation in proper solvents by moderate heating,[65,66] which result in adjustable textural properties and mesoporosity by changing precursor concentrations.

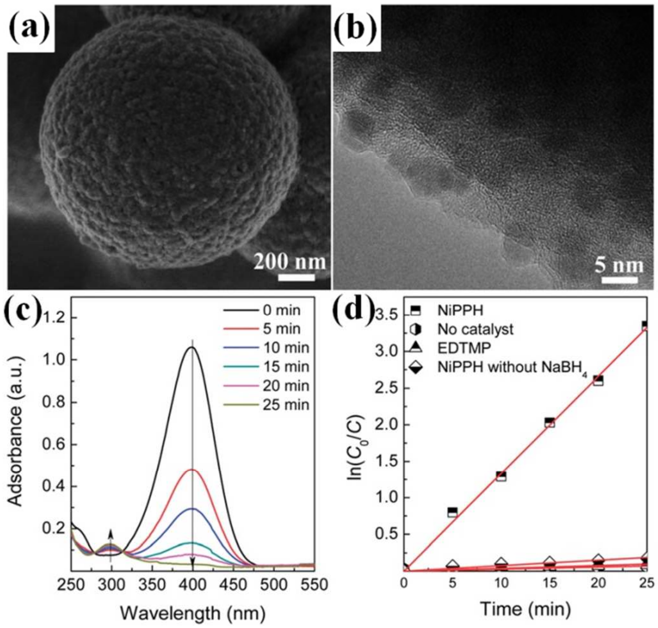

Fig. 2 SEM (a) and TEM (b) images of mesoporous nickel phosphate/phosphonate material, marked as NiPPH, the embedded nanoparticles are crystalline nickel phosphate. Time-dependent UV-vis absorbance spectrum for the catalytic hydrogenation of 4–nitrophenol to 4–aminophenol in the presence of NiPPH and NaBH4 (e) and plot of ln(C_0/C) versus reaction time (f).[64]

Sol–gel chemistry templated by the formation of micellar lyotropic assemblies generated by the amphiphilic precursors have been widely adopted to prepare mesoporous materials.[67] The unique hydrolysis properties of metal alkoxies and alkylmetals with or without co-reactant depending on the desired chemical compositions can lead to the fantastic porosity even under relatively mild conditions.[68-70] Hierarchically mesoporous titanium phosphonates of mesostructured cellular foam pore were synthesized using tetrabutyl titanate.[47] Indeed, the microemulsion generated from the hydrolysis of tetrabutyl titanate in the multicomponent system of water–alcohol–phosphonic acids served as the role of porogen. Different sorts of organophosphonic acids would influence the interfacial polymerization behavior and thus the resulting micro-morphology. Mesoporous titanium oxide–phosphonate nanorods could be synthesized while using alkyl diphosphonic molecules.[48]

During the self–assembly processes, the synthesis parameters are of significance in influencing the structural properties of the mesoporous metal phosphonates. Diverse weak interactions at the molecular scale propel the template–free assembly to give mesoporous metal phosphonates. Regardless of the synthetic simplicity, the synthesis processes are difficult to control to some extent and this way cannot afford the valid capability to adjust the porosity, texture, and even morphologies on demand. A more controllable method is required from the viewpoint of research and practical applications.

2.3 Surfactant assistance for uniform mesopore channels

The synthesis methodology of periodic mesoporous materials features the templating concept that was proposed over twenty years ago. The template–induced route for the formation of mesopores can be devided into two categories. The first one is so–called hard templating. The prerequisite point of this way is the preformed ordered mesoporous materials with rigid or semi-rigid frameworks. Alternately, the negative replica of the templates can be obtained after the filling of precursors into the void spaces. Especially, the template removal requires harsh conditions such as calcination and strong acid or base treatment, making it technologically cockamamie, environmental unfriendly, and not apposite for preparing mesoporous organic–inorganic hybrid materials.[34,35,71,72] By contrast, the soft templating approach is more versatile, flexible and effective. The self-assembly that happens during soft templating is a remarkable phenomenon that initiates the structuring of surfactants, precursors, and solvent molecules, and thereby, the mesostructures can be tuned through controlling system parameters, solvents and the nature of the supermolecular template molecules.

It should be noted that the high hydrolysis rate of metallic precursors cause microphase separation in most situation. Recent study has illustrated the functions of pH value and temperature in impacting the condensation and polymerization. Under extremely acidic conditions, the relatively controlled reaction speed could benefit the formation of hexagonal aluminum phosphonate mesophases after slowing evaporating the solvents at room temperature.[51-53] However, the less condensed and easily hydrolyzed frameworks made extraction of as-synthesized hybrids by mild acid treatment unworkable. Low temperature calcination was carried out but it might introduce impurities and destruct mesophases. Increasing the pH value to around 4, the hydrolysis speed of inorganic precursors accelerated while a cryosel bath could create low-temperature conditions for slowing down the hydrolysis and condensation of the reactants.[38,39,54]

Metallic precursors can be pretreated with some ingeniously selected organic reagents to alleviate the hydrolysis and improve the interactions with surfactant micelles. Dissolving metal cholorides or nitrates in alcohol could produce metal alkoxide analogies but with several times slower hydrolysis rate,[73,74] and ethanol with moderate polarity was usually used. A chelating polyalcohol, 2,2',2''-nitrilotriethanol (TEAH), could complex aluminum atoms, thus proving its capability of harmonizing the rates of the hydrolytic reactions of the aluminum species in water–phosphonic acid media and the subsequent processes of self–assembly among the resulting inorganic polyanions and the surfactant aggregates.[75-77] And a series of mesoporous aluminum monophosphonates and diphosphonates were successfully synthesized on the basis of this "atrane route".[76,77] In addition to the alcohols, crown ethers of hydrophobic alkyls not only could capture metal ions to effectively isolate the innerly embedded metal cations from the organic functionalities and thus to slow down the reaction rate, but also allowed the assembly between surfactants and hybrids, as well as the surrounding coordination expansion.[78,79]

A great deal of progress has recently been made in the field of mesoporous metal phosphonates. Unlike mesoporous silicas and carbons, the rational synthesis of metal phosphonate hybrids with uniform mesopore channels is a burgeoning area. The rapid hydrolysis of metallic species and strong coordinating ability of the organophosphonic groups prompt us to find the right ways to weaken these effects as far as possible, such as accomplishment via changing synthetic conditions and adding organic chelates. It should be kept in mind that the key factors for the efficient assemblies of periodic mesophases include the control of the aggregation of precursors, sufficient interactions between oligomers/precursors and surfactants, and a suitable size and charge of the building blocks. Additionally, different mesostrucures lead to distinct physicochemical characters and thereby the catalytic performances, though realizing mesostructure regulation is still a challenge in preparing periodic mesoporous hybrid materials. This may be due to the fact that the incompletely condensed hybrid network, the complex coordination chemistry between metal ions and organic bridges and the weak interactions among the organic components may converge to form relatively stable hexagonal phases.[54,80-84]

A variety of surfactants are capable of templating different mesopore sizes, which are determined by hydrophobic/hydrophilic volume ratio of supermolecules. Ionic and oligomeric surfactants generally produce small mesopores in the range of 2–5 nm.[26,27,51-53,76,77,85,86] Higher molecular weight Pluronic block copolymers can template mesopores of 6–10 nm in diameter,[39,51] even larger mesopores using polystyrene–block–poly(oxyethylene) colloidal templates. Note that judicious choice of suitable synthetic technologies would result in various types of mesostructured micromorphologies, such as nanospheres, nanofibers and films, of which the pore size could be precisely controlled by the involved soft supermolecules. Nonetheless, the shortcoming of surfactant–assisted route is also apparent, *i.e.*, the pore size are limited within the tens nanometers, while sol–gel chemistry can create pores in the macroporous region though the uncontrollability. Micelles and liquid crystals are virtually dynamic that are readily altered when changes are occurred in the surrounding conditions. Addition of aromatic or aliphatic hydrocarbons causes the swelling of micelle cores up to a point, which is one way to increase pore size in soft templating.

3. Heterogeneous catalytic applications

The catalytic applications of mesoporous metal phosphonates have been investigated in the past years. In this section, we discuss the potentials in oxidation, hydrogenation, addition, assymetric catalysis, electrocatalysis, and so on, which are presented based on metal sites, phosphonate groups, and the derivatives of metal phosphates. These are summarized in **Fig. 3**. Some recent progress is presented as follows.

3.1 Metal site based catalysis

Transition and some main group metal elements are typically considered as an outstanding metal centers to build metal phosphonate skeletons, which is due to the valuable capability of gain and loss of electrons and/or the corresponding apparent redox ability. Notably, the water solubility of metal

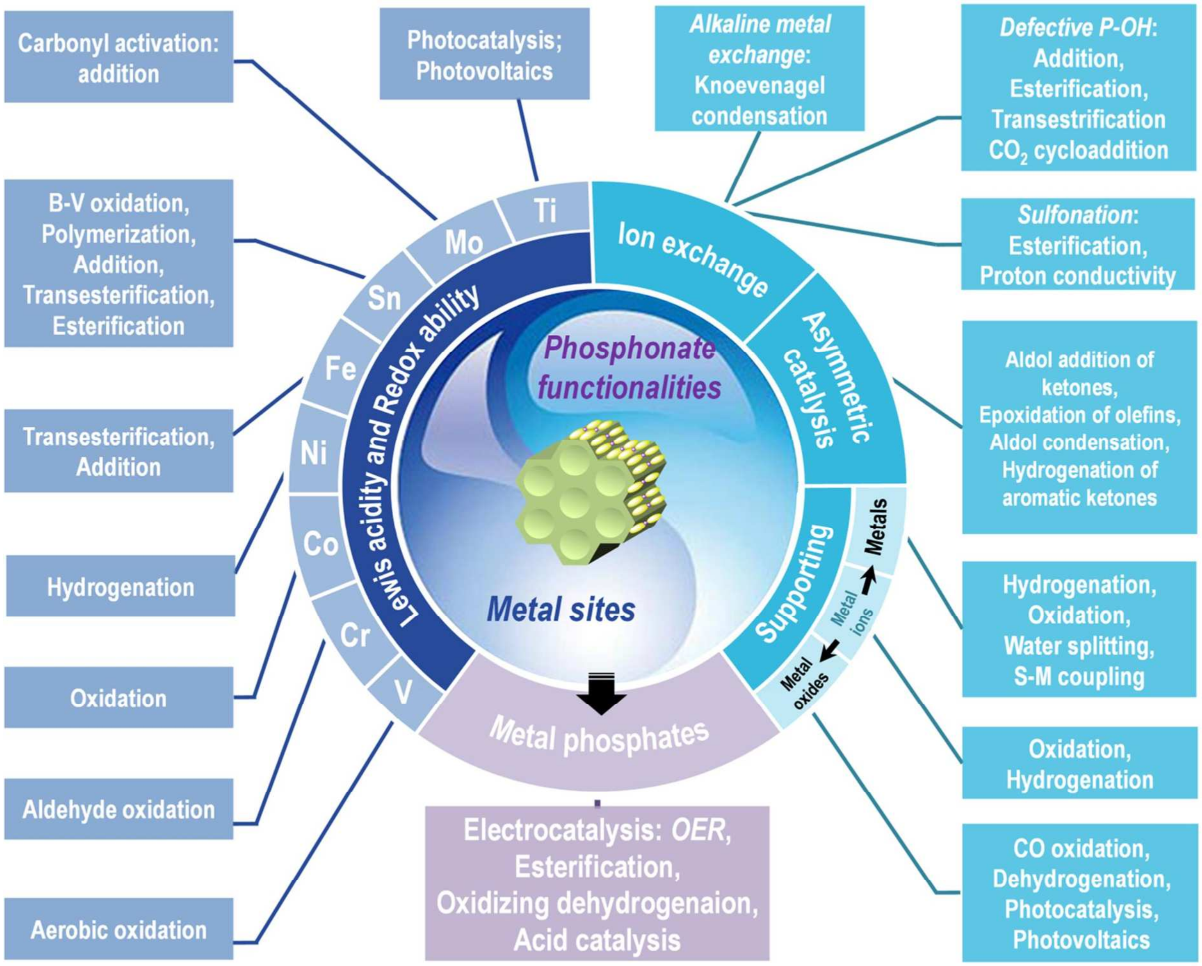

Fig. 3 A summary of potential heterogeneous catalytic reactions of mesoporous metal phosphonate materials.

phosphonates decreases with the increase of the valence of the metals.[92] As to trivalent and tetravalent metal phosphonates, the considerable insolubility and stability permit the use in harsh conditions.

3.1.1 Photocatalysis. Much attention has been directed to titanium oxide–based photosensitizers for environmental remediation and energy conversion purpose. In response to the unfavourable band gap of titanium oxides, foreign element doping is an alternative route to extend light absorption range and to reduce the recombination probability of photoinduced electron–hole carriers. Since a variety of guest species can be introduced into the titania framework by using phosphonic acids, mesoporous titanium(IV) phosphonates are suggested to perform well in photocatalysis. With ethylene diamine tetra(methylene phosphonic acid) (EDTMP) being the organophosphonic linker, the band gap value of the hierarchical macro–/mesoporous titanium phosphonates showed an obvious narrowing comparing with that of pure titania.[93] The shift of the absorbance onset towards the lower energy region indicated that the titanium phosphonate materials might make a better use of the solar light, resulting in enhanced performance for organic dye decomposition. pH value of the synthesis systems was an important factor to tune the band gap energies owing to that the pH condition could affect the polymerization rate of precursors and the condensation degree of the final hybrid frameworks. A weak alkaline condition caused an inferior photoactivity due to a small surface area.[93] The red shift of the absorbance edge of titanium phosphonates as the homogeneous doping of phosphonic moieties demonstrate an impressive photocatalytic behavior.

Hexagonal mesoporous titanium phosphonate synthesized with the assistance of surfactant was proven to be an efficient photocatalyst under light stimulation[94] in comparison with the phosphonates prepared in the absence of surfactant[93]. This improvement was attributable to the enhanced absorption in visible light range and the periodic mesoporosity together with a high surface area, which could provide more active adsorption sites, and thereby increase the efficiency of photoabsorption through multiple scattering and improve mass transfer across the mesopores.[95] Interestingly, after treating with a mixture of organic dyes and heavy metal ions, mesoporous titanium phosphonates showed an even higher activity for the destruction of organic dyes (**Fig. 4**).[94] This could be due to the formation of complexes of metal ions on the surface of the hybrid network, resulting in a new broad absorption peak emerging in the visible light region. This could thus give rise to a better use of visible light. Also, optimization of the channel structures of mesostructures signifies a crucial way to elevate the catalytic activity.[41,96] Cubic mesophases possess finely interconnected pore systems as compared with the hexagonal ones. By changing the molar ratio of the adding amount of surfactant and inorganic precursor, the different phases of the mesopores could be transformed into each other,[54] and the resultant cubic mesoporous titanium phosphonates could be employed as useful photocatalysts for the degrading organic contaminants. These materials are suitable catalysts because of the homogeneous incorporation of phosphors and carbon and large surface area of well–structured mesoporosity.

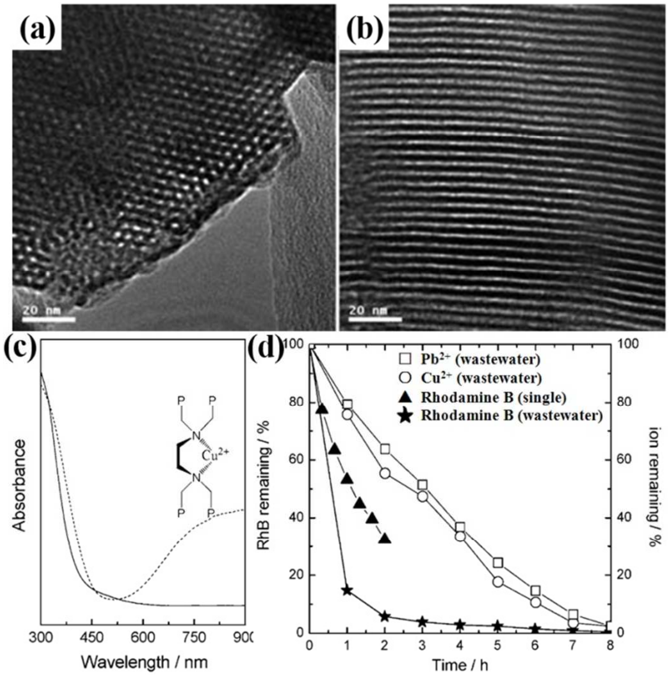

Fig. 4 (a, b) TEM images of periodic mesoporous titanium phosphonate (PMTP-1). (c) UV/Vis diffuse-reflectance spectra of PMTP-1 before (solid line) and after Cu^{2+} ion loading (dashed line); b) one-pot heavy metal ion adsorption in the wastewater treatment as well as Rhodamine B photodegradation by using PMTP-1 under simulated solar light irradiation.[87]

One step further based on phosphonate–mediated photocatalysis is to find their qualification as photoanode materials in photoelectrochemical field, in which photogenerated electrons transfer to external circuit while separated holes from photosensitizers act as oxidants to oxidize electrolytes. Titanium phosphonate material with a mesoscopic void space and a self-assembled nanostructure was synthesized using conjugated benzene–1,3,5–triphosphonic acid.[97] Photosensitizer molecule (Rose Bengal) could be loaded into the mesopores via impregnation, demonstrating higher carrier mobility for photocurrent generation than other titanium oxide based nanomaterials. The traditional preparation of the dye–sensitized electrodes of solar cells is accomplished by the adsorption of dye molecules onto the pre-synthesized semiconductor membranes, which usually leads to a very low loading amount of the photosensitive molecules.[98] The overincreasing of the loading amount would cause the dye aggregation, and the poor contact between the aggregated dye molecules and the photoanode materials could prohibit the transmission of photoelectrons. The sol–gel method allowed the molecular–level penetration of large π–aromatic photosensitive groups, such as phthalocyanines with sulfonic or phosphonic acid groups, into the mesoporous network of photoanode materials homogeneously and the achievement of an unprecedented high loading amount of organic dyes, resulting in an significantly large loading amount of organic dyes, but without the disadvantages of dye aggregation and poor electron transmission caused by the isolation of single–dye centers by the surrounding semiconductor oligomers.[99] The resultant mesoporous hybrids were proven to be efficient photocurrent conductors and better electrode materials than the traditional dye–modified titania materials under the same experimental conditions. Stability is a key index as well from the practical solar cells point of view. Phosphonic linkers were found to represent a promising alternative due to their higher affinity towards the surfaces of metal oxide semiconductors and stronger binding ability than carboxylic grafting groups,[100,101] and they would thus give better long–term stability of DSSCs.

3.1.2 Carbonyl activation. Recently, tin–doped molecular sieves could selectively activate carbonyl groups for oxidizing due to the proper Lewis acidity.[102-104] The Baeyer–Villiger (BV) oxidation is the oxidative cleavage of a carbon–carbon bond adjacent to a carbonyl, converting ketones into more complex and valuable esters and lactones. Mesoporous tin phosphonate materials were testified to be of outstanding efficiency for BV oxidizing reactions in the presence of suitable oxidants.[105,106] The most fascinating portion of these hybrid catalysts was that the reaction proceeds efficiently in the absence of any organic solvents since the use of hazardous and ecologically unattractive organic solvents would produce carboxylic acid salts as the byproduct. Tin phosphonates with surface areas less than 400 m^2 g^{-1} could catalyze BV reaction in the presence of H_2O_2 to give high conversion and selectivity, for example, the conversion of cyclohexanone was 68%.[105] Increasing the surface area could boost the catalytic activity. Without using any peroxide, micro– and mesoporous tin phosphonates with a high surface area of 723 m^2 g^{-1} could achieve a relatively higher yield of 74% with respect to the initial cyclohexanone with the help of molecular oxygen.[106] There was no perceivable change in the activity of the catalysts during the recycling tests, revealing the stability of the heterogeneous hybrid materials. In the case of Hantzsch ester synthesis reaction to produce 1,4-dihydropyridines,[107] an important biological activity in the treatment of cardiovascular disease, the (C=O) group of the α,β–unsaturated carbonyl compound could be activated by the positively charged metallic Sn on the hybrid pore walls that simultaneously increase the nucleophilicity of C=C, leading to formation of 1,4-dihydropyridines with exclusive selectivity over 2-arylpyridines or 1,2-dihydopyridines under mild conditions.[108]

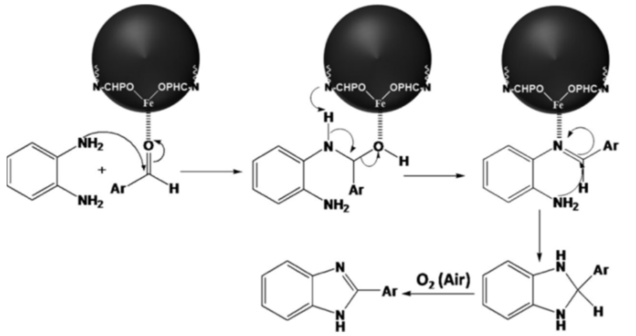

Fig. 5 Supposed mechanism for the synthesis of benzimidazoles. The iron center in the catalyst activated the aromatic aldehyde and facilitated the attack of the amine. The tertiary amine groups in the catalyst helped to eliminate the protons in the water-removal step. The iron center activated the molecule for the second attack of the amine. Thus, the cooperative involvement of iron and the tertiary amines in the catalyst catalyzes the synthesis of benzimidazole derivatives.[110]

Mesoporous self–assembled hybrid molybdenum phosphonate nanomaterials showed high catalytic activity and recycling efficiency in the green and efficient one-pot condensation reaction for the synthesis of bioactive 2-aryl benzimidazoles by the condensation of *O*-phenylenediamine and substituted aromatic aldehydes in excellent yields at room temperature, in which the molybdenum(V) with vacant d orbitals in the hybrid framework played the crucial role for activating the carbonyl carbon of the substituted aldehydes.[109] The corresponding high yield was positively correlated with the surface area. As the surface area reduced, the mass transport through the porous channel was obviously impeded, which is reflected in the isolated yield of the product. Moreover, the number and uniformity of the active catalytic sites increased gradually with the decrease of the particle size. By contrast, iron phosphonates materials were catalytically active towards the synthesis of benzimidazole derivatives (**Fig. 5**),[110] but with a lower activity comparing with the molybdenum phosphonate counterparts[109]. This might be related to the moderate Lewis acidic strength of molybdenum due to the larger atomic radii than that of iron atoms. It was speculated that the interaction between the catalyst and the carbonyl oxygen was strong enough to subsidize the effect of the substituents, while the amine groups of *O*-phenylenediamine were attached onto the carbonyl carbon.[109] The tertiary amine groups could help to eliminate the protons in the water-removal step, and this synergistic effect of the iron center and the tertiary amine groups catalyzed the synthesis of benzimidazole derivatives.

Environmentally friendly biodiesels are appropriate substitutes for the traditional fossil energy in terms of sustainable development. Generally, biodiesels can be produced through acid-catalyzed esterification of long chain fatty acids with alcohol and base promoted transesterification.[111] Nevertheless, industrial processes using homogeneous catalysts are confronted with intractable drawbacks because of substantial generation of byproducts and neutralization and separation problems.[112] It is pertinent to mention that organic–inorganic iron phosphonate could fit the qualification in catalytic transesterification reactions under solvent–free conditions.[113] It was proposed that the electrophilicity of the carbonyl carbon of the reactant ester group was the main driving force of the reaction. The conversion to the lower alkyl–substituted ester lowered with the decrease of the electron–withdrawing effect of the substituent to the ethyl–substituted acid group. Further optimization of the mesoporosity of iron phosphonates through surfactant-assisted strategy may improve the mass transport capability so as to improve the apparent catalytic performance.[114,115] Indeed, mesoporous tin phosphonate hybrids with crystalline pore walls performed well for catalytic esterification of long chain fatty acids with methanol under mild reaction conditions.[116] The catalytic reactions were found to be much faster as compared with homogeneous and heterogeneous tin based catalysts.[112] On one hand, the surface Lewis acidity made contributions to the catalytic activity; on the other hand, the suitable polarity of the crystalline pores would facilitate the diffusion of polar methanol molecules across the mesopores[39].

3.1.2 Catalytic hydrogenation and oxidation. Inspired by the catalytic hydrogenation reactions using nickel nanosols as catalysts,[117,118] mesoporous nickel phosphonate materials were explored to reduce nitroarenes to anilines in the presence of sodium borohydride as reducing agent much recently.[64,119] According to the nickel phosphate–mediated self–assembly process, the synthesized mesoporous nickel phosphate/phosphonate microspheres exhibited excellent capacity for catalytic hydrogenation of 4–nitrophenol to 4–aminophenol under ambient conditions (**Fig. 2c** and **d**),[64] which was even comparable with some noble metal nanocatalysts[120]. The good hydrogenation capability was also confirmed by the reduction of 5–nitroisophthalate to 5–aminoisophthalate.[119]

Within the same group as nickel in the Element Periodic Table, cobalt phosphonates were found to efficiently decompose organic contaminants with sulfate radicals of considerable reaction kinetics and thermodynamics.[121] Therein the tightly integrated divalent cobalt inside the hybrid networks exhibited strong activity towards activation of peroxymonosulphate to generate sulfate radicals, which possessed more powerful oxidizing ability towards the decomposition of organic molecules as compared with hydroxyl radicals from H_2O.[122] The difference between the two radicals lay in the abilities of their redox partners as leaving groups, whereas the bisulfate and sulfate ions are for the sulfate radical and the water molecule for the hydroxyl radical. And the hollow microstructures resulted from self–templated microemulsion effect[121,123] presented abundant active sites and thus promoted efficient adsorption and diffusion of reaction molecules to show a superior catalytic efficiency. The mechanism of heterogeneous catalysis was considered to involve a single electron transfer process, the oxidation of Co(II) with peroxymonosulfate and the formation of sulfate radicals as well as the reduction of Co(III) and the generation of peroxymonosulfate radicals.

Nonetheless, the mild oxidizing ability of H_2O_2 makes other porous metal phosphonates become potential heterogeneous catalysts for oxidation of aldehydes and olefins. Organic–inorganic hybrid tin phosphonate material with mesoporous voids could effectually catalyze the radical polymerization of styrene at room temperature in the presence of aqueous H_2O_2 as an initiator under solvent–free conditions, whereas in the presence of aprotic solvent it facilitated partial oxidation of styrene.[124] The stability of the hydroxyl radicals formed during the polymerization reaction played an important role in the polymerization of styrene, and the absence of solvent could stabilize the hydroxyl radicals as the acidic nature of neat H_2O_2. The possible formation of tinhydroperoxo species at the hybrid surface in the presence of aprotic solvent and H_2O_2 could facilitate the partial oxidation of styrene via initial epoxidation to styrene oxide, [125,126] which underwent rearrangement and further oxidation to yield phenyl acetaldehyde and acetophenone.

Chromium oxophenylphosphate of fine microporosity and mesoporosity showed good catalytic activity in the liquid phase partial oxidation of aldehydes to the respective acids in the presence of dilute aqueous H_2O_2 as oxidant at room temperature, accompanied with certain stability after three times cycling experiments.[127] In the presence of both catalyst and peroxide there was about 70% conversion of cinnamaldehyde.

Mesoporous vanadium phosphonate material, constructed from a multidimensionally dendritic tetraphosphonate without the use of any surfactant, could perform as an excellent catalyst for the aerobic oxidation of benzylic alcohols with high reactivity and shape selectivity.[128] The oxidation generally proceeded very smoothly with the formation of corresponding benzylic aldehydes with high conversion and selectivity. Neither benzoic acid, a product of benzaldehyde overoxidation, nor ethers from acid condensation of the benzylic alcohol substrates, were found in significant amounts as products in the reaction mixture.

A functional pore system with various metal nodes offers an invitation to use these nanoconfined spaces as nanoreactores, thus creating advanced mesoporous nanocomposites with rationally contrivable interfaces. In general, the catalytic activity mainly originated from the homogeneously distributed metal sites in the hybrid frameworks is intimately relevant with the strength of Lewis acidity and the redox potential of metal elements with multiple valences. Some mesoporous metal phosphonates have shown comparable catalytic acidity to the corresponding homogeneous metallic catalysts, which are sometimes inspired by the catalytic characteristics of metallic salts and their coordination compounds, metal oxides and phosphates. A second metal center is reasonably to be introduced into the phosphonate networks, and the mesoporous hybrids with dual metals may facilitate the catalytic applications due to the improved features by more than one functional composition. The unique interactions of metal–metal and metal–support may evoke an interesting catalytic activity and stability. However, up to date, although a great diversity of phosphonate hybrid materials with various metallic nodes have been prepared on the basis of the gradually established metal phosphonate chemistry, catalysis supported by metal phosphonate materials remains in its infancy. Modifying and matching different factors to obtain further improvement of the catalytic activities and to achieve a wider scope of catalytic properties has always been the aim of the synthesis of metal phosphonate heterogeneous catalysts.

3.2 Catalysis based on the phosphonate groups

The interesting coordination chemistry of phosphonate ligands and the diverse types derived from nature or human synthesis have endowed mesoporous metal phosphonates with extensive capabilities for catalysis including acidity/alkalinity and hydrophobicity/hydrophilicity. It is viable to yield chemo-, regio-, stereo- and/or enantioselectivity in the restricted space available. The post-modification on the integrated phosphonate bridging groups makes this area even further and deeper.

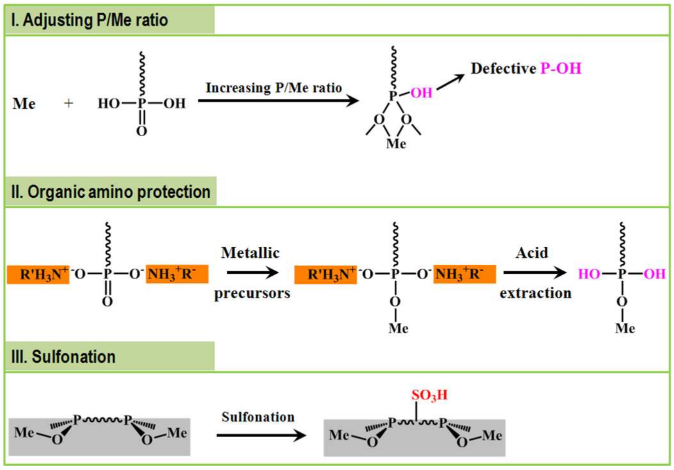

Fig. 6 A summary of the general routes to enhance the ion exchange ability of mesoporous metal phosphonates hybrids.

3.2.1 Ion exchange. Ion-exchange materials are very common for inorganic materials such as aluminosilicate zeolites, and attempts to realize the exchange of cations or anions can make the resultant catalyst suitable in the fields of environment–friendly catalysis.[129,130] General approaches to adjust the ion exchange ability of mesoporous matel phosphonates are illustrated in **Fig. 6**. For mesoporous metal phosphonates, the H^+ exchange capacity was usually limited in the conventional synthesis methods. Note that the H^+ exchange of these materials stem from the defective P–OH groups in the resultant solids,[12] while the condensation between P–OH and metal ions often resulted in the extensive formation of P–O–Me (Me = Ti, Zr, V, Al, Sn, Fe, *etc.*) bonding mode instead of defective P–OH.[131] The H^+ exchange capacity reflect the acid content substantially, and acid content is one of the key elements to weigh the catalytic activity and efficiency. One simple route to increase the exchange ability is to regulate the molar ratio of the inorganic and organophosphonic precursors.[113] The atomic ratio of P and Fe could be varied from 0.50 to 0.59 in the series of the synthesized iron phosphonates by changing the P/Fe ratio in the range of 1 to 4. The uncoordinated phosphonic groups would exist in the form of defected P–OH in the porous architectures. The actual ion exchange capacity could be determined by titration curve using NaOH. Mesostructured zirconium organophosphonate synthesized with the assistance of the surfactant cetyltrimethylammonium bromide (C_{16}TABr) displayed an ion exchange capacity of 1.65 mmol g^{-1}, which was active in the acid-catalytic synthesis of methyl-2,3-*O*-isopropylidene-*β*-D-ribofuranoside from D-ribose.[132] This catalytic performance was comparable to that of liquid acid HCl and commercial ion-exchange resin NKC-9. The excellent catalytic activity could be attributable to the high surface area, which was beneficial for the distribution of the active sites and for their exposure so that they can readily be attached by the reactants, and the mesopores aided in the acceleration of mass transfer.

However, it is quite limited for increasing the H^+ exchange capacity of the resultant mesoporous metal phosphonates by adjusting P/metal ratio.[133] In order to achieve a high concentration of acid amount in the desired metal phosphonates, a series of alkyl amines were used as protecting groups during the condensation process, based on the reversible reaction between alkyl amines and P–OH groups in the phosphonic bridging molecules.[134] The alkyl amines first partially occupied the P–OH sites by acid–base reactions, followed by the condensation between the added alkoxides and residual P–OH and P=O groups. Extraction with HCl finally released the P–OH defects of the resultant solids, leading to a high acid content. But in the absence of amines, the P/Ti ratio reached a plateau of 1.35–1.51 when the added P/Ti ratio was larger than 1.75, due to the limit of coordination ability of titanium with phosphonic acids. When ammonia was used instead of alkyl amines, the enhancement effect was hardly detected, probably because inorganic amine was too volatile to form relatively stable bonding with P–OH in the competitive reaction with alkoxides. Remarkably, the resulting ion exchange abilities was much higher than other counterparts synthesized via other conventional methods.[108,113,124,132] Taking the condensation reaction of D-ribose with methanol and acetone as an example, the yield of methyl-2,3-*O*-isopropylidene-*β*-D-ribofuranoside outperformed mesoporous zirconium phosphonate,[132] implying the effectiveness of the organic amine pre-protection. On the contrary, after being treating with NaOH aqueous solution, zirconium phosphonates could be used as solid base catalyst for Knoevenagel condensation of benzaldehyde with diethyl malonate or malononitrile, cyclohexanone with malononitrile under mild reaction conditions, presenting high catalytic activity with valuable stability and recyclability.[135]

The exclusive use of mesoporous metal phosphonates based on ion exchange can be promising in cycloaddition reactions that involves the small−membered ring compounds and CO_2, such as aziridines to oxazolidinones and epoxides to cyclic carbonates, both of which are vital intermediates for producing industrial and pharmaceutical chemicals. Carboxylate metal−organic frameworks (MOFs) could catalyse these cycloaddition reactions.[136-139] With the analogous hybrid networks of higher stability, the defective P–OH of mesoporous zirconium phosphonates could activate aziridine molecules, followed by a nucleophilic attack of CO_2 to produce the carbamates, showing outstanding activity, selectivity, and recyclability.[140] The amino groups incorpored in the phosphonate linkages could activate the inert CO_2, thus boosting the reaction conditions and lessening reaction time, while preserving high conversion, yield, and regioselectivity.[141] In other words, bifunctional hybrid catalysts containing moderate Lewis acidic and basic sites are preferred in the CO_2 cycloaddition reactions.

However, the further application of pristine metal phosphonates may be confined to the finite open metal sites and weak functional organic sites to a certain extent. Some of functionalization methods have been applied on the mesoporous metal phosphonates to achieve high acid content and acid strength for efficient acid catalysis. Owing to the hybrid natures, the organic fragments could be easily tailored by applying classical organic chemistry, for example, the sulfonation of alkyl or aryl groups in mesoporous metal phosphonates.

It has been amply demonstrated that mesoporous phosphonates, constructed from phenyl- containing phosphonic acids, are readily sulfonated.[142-145] In the anhydrous state the sulfonated porous biphenylphosphonates have been shown to be a near superacid with roughly the acid strength of concentrated sulfuric acid,[142] making them applicable for esterification reaction. The sulfonated mesoporous zinc phosphonates possessed high activity and recycling efficiency for the synthesis of different biodiesel compounds via esterification of long chain mono and bicarboxylic acids by using methanol as both reactant and solvent at room temperature.[145] Ordered mesoporous titanium phosphonate hybrid materials were functionalized by sulfonation with chlorosulfonic acid to form stable hydrosulfated esters, indicative of a strong solid acid,[146] showing a much higher conversion (87.3%) than the unfunctionalized materials (4.9%) in the esterification of oleic acid and methanol for biodiesel production under ambient conditions. The relatively milder esterification condition involving the grafted sulfonate groups than that of pristine metal phosphonate Lewis acid catalysts could correspond to the stronger acidity of Brönsted acid sites.[147,148]

From the viewpoint of sulfonate−mediated catalytic mechanism, the sulfonation route would increase the hydrophilicity and create a slight positive charge on the carbonyl carbon by protonating the adjacent oxygen atom. The nucleophilic alcohol attacked the activated carbonyl carbon, thus producing water and esters. In fact, the hydrophobicity and hydrophilicity of the mesoporous metal phosphonates can be intentionally tuned by incorporating different organophosphonic linkers,[149,150] and as such, the catalytic activity and selectivity that are only confined to acid catalysis can be rationally adjusted to some extent. On the other hand, the stability of mesoporous metal phosphonate, due to the solid coordination between the phosphonate groups and metal atoms, makes them potential as water–tolerant catalysts such as ester hydrolysis.[34,35,146,151,152] From the aspect of sulfonation process, the limited chemical stability of metal phosphonate hybrids does not enable harsh functionalization conditions as the risk of destroying the framework. In this sense, the use of acid-bound agents, such as pyridine[146] and triflic anhydride[153], could circumvent this drawback of hybrid framework sensitivity and sulfonate the mesopore surfaces at the same time.

3.2.2 Supported catalysts. The organophosphonate bridging moieties can immobilize a great many of metal ions on the basis of host−guest acid−base interaction. Combining with the mesoporous structures and large surface areas, a novel type of metal phosphonate−based supported catalyst can be envisioned. After Fe^{3+} was intercalated and coordinated with nitrogen and carbonyl groups inside the porous walls, the Fe^{3+}-incorporated zirconium phosphonate could be used as catalyst for oxidation of formaldehyde in the presence of hydrogen peroxide,[154] wherein the loaded Fe^{3+} could activate H_2O_2 to produce highly oxidative hydroxyl radicals[125,155-157] towards formaldehyde oxidation[154]. Similarly, immobilization of Co^{2+} on periodic mesoporous aluminum phosphonate could realize the heterogenization of homogeneous high-performance modified Fenton reaction for oxidizing decomposition of organic contaminants (e.g. such as phenol) in the presence of peroxymonosulfate.[149] Likewise, noble metal ions could be immobilized onto the hybrid surface.[158-160] Pd^{2+}–complexed zirconium phosphonate materials possessed good activities for the hydrogenation of the carbon–carbon double bond.[160] Here the hydrogenation reactions were carried out easily in some solvents with intermediate dielectric constant including alcohol, acetone and especially methanol. But the palladium complexes lost their catalytic activities for hydrogenation in some solvents with high or low dielectric constant such as glycol and chloroform. The solvent effect might be assigned to the solubility and mutual solubility of catalytic centers in the palladium complexes.

Noble metals have been known for their catalytic performances. What is noteworthy is that the coordinated noble metal ions can be further reduced to nanoparticles or nanoclusters within the porous metal phosphonate matrixes.[159,161,162] Encapsulation of noble metal nanoparticles inside the metal phosphonate frameworks may extend their applications in catalysis by catalytic spillover. The size of loaded nanoparticles could be controlled by the synthesis techniques, *i.e.*, reductant types and annealing temperatures.[161] Large particles could be attempted with the use of alchohol, while calcination would prefer small particles. The binding sites were no longer occupied after reduction and available for further coordination. Increasing the reduction temperature had no evident effect on the final size of the nanoparticles, signifying that their growth was limited by the pore structure of the phosphonate matrix that would prevent nanoparticles from aggregation.[161] This provides a simple way to control the size of the loaded active components. Colloidal Pt has been found to be an ideal catalyst for the reduction of water to hydrogen gas.[163,164] The Pt nanoparticles inserted in the phosphonate substrate produce hydrogen photochemically from water under ultraviolet light illumination.[159] The average rate of H_2 production was 0.15 mL h^{-1} with a lower limit quantum yield of 4% based only on the ultraviolet portion of the spectrum in the presence of a sacrificial reductant. Disappointedly, the usefulness of these materials is limited to UV light, and the strong UV light eventually destroyed the system after long-term exposure. It is urgently required to optimize the system and to design materials that absorb in the middle of the visible spectrum.

The homogeneous arrangement of phosphonate functional groups inside the hybrid walls realizes the monolayered adsorption behaviour for metal ions with high uniformity.[38,54,64,87,118,123] Also, the doping effect of organophosphorus sources can extend the absorbance spectrum of titanium oxide to visible light region.[47,93,133] Furthermore, the construction of heterojunction structure at the semiconductor interface is suggested to enhance the separation efficiency of photogenerated electron−hole pairs during the photocatalytic process.[17,20,165,166] Thereafter, mesoporous phosphonate-titania hybrid materials were prepared with the use of ATMP as the grafting group and triblock copolymer F127 as the template.[167] The homogeneously anchored ATMP on the mesoporous wall allowed monolayered adsorption of Zn^{2+} by extensive coordination. Highly dispersed photoactive ZnO nanoparticles were then formed through the reaction with stoichiometric NaOH and a low–temperature annealing procedure (**Fig. 7a**). The resultant ZnO coupled mesoporous phosphonated titanium oxide photocatalysts exhibited better photocatalytic activity and stability in the photodegradation of Rhodamine B under both UV and visible light irradiation than those of pristine mesoporous phosphonate titania, commercial titania P25, and mesoporous ZnO/titania. Similarly, the adsorbed metal ions could be directly oxidized to active metal oxides through high–temperature calcination, and the final supported materials could find their use in the area of catalytic oxidation.[168,169] To make a high allocation of CuO nanoparticles, the Cu^{2+}-saturated hexagonal mesoporous titanium phosphonate microspheres with a high thermal stability was experienced a high-temperature calcination process with the periodic mesostructures being hardly destroyed (**Fig. 7b**).[170] The density and distribution of the surface organic functional groups could be tuned, which permitted a facile adjustment of the dispersion of the Cu^{2+} and the final CuO loading contents. Catalytic CO oxidation was taken as the probe reaction, and the CuO-supported mesoporous titanium phosphonates presented high catalytic activity and significant stability.

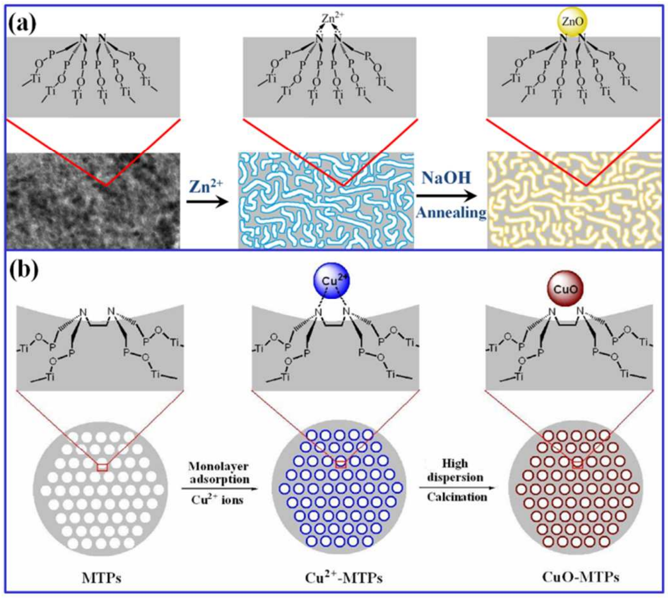

Fig. 7 (a) Simulated formation mechanism of ZnO on mesoporous phosphonated titania[167] and (b) CuO on periodic merosporous titanium phosphonate hybrid.[170]

Metal ions or their derivatives including metals and oxides can be loaded on mesoporous metal phosphonates, in which the coordination interaction initially promotes the supporting process and the homogeneous organic units allow for uniform dispersion. The strong interaction between hybrid supports and active components ensures the stability of the coupled catalysts. The high specific surface area and tuneable pore size make the loaded active components adjustable from the view of amount and size. With regard to photocatalysis, metal sulfides and selenides generally own narrower band gap comparing with oxides, making sulfides and selenides promising in environmental remediation and photoelectric conversion on condition that they are immobilized on suitable mesoporous metal phosphonate nanocomposites.

Although heterogeneous catalysts show superiorities in stability and reusability, it should not be neglected that the inferior catalytic activity in comparison with homogeneous catalytic systems. Consequently, based on the organosolubility of zirconium phosphonates designed recently,[171-173] a novel type of recoverable and reusable zirconium phosphonate-supported Pd catalysts was reported using the concept of one-phase catalysis and two-phase separation (**Fig. 8**).[174] The original zirconium phosphonates were readily soluble in $CHCl_3$ and THF, whereas supported Pd catalysts were only soluble in THF, and thus homogeneous catalysis was achieved in THF and the catalyst could be recycled by means of solid/liquid separation upon the addition of poor solvents such as petroleum ether after the completion of reaction.[175] The organosoluble properties made them suitable for homogeneous Suzuki–Miyaura coupling reactions of various substituted aryl bromides with arylboronic acids. Attractively, due to their organosolubility, homogeneity and small size of Pd particles embedding in the zirconium phosphonate matrix, the supported palladium catalysts possessed high catalytic activities even at room temperature. This method can be easily extended to other metal catalysts.

Currently, mesoporous metal phosphonates have been specialized functionality as a new category of materials for bioapplications, such as biosensoring, bioimaging, drug delivery, and immobilization of enzymes and proteins.[26,27,123,150,176-181] Remarkably, enzymes are natural catalysts, featuring high reactivity, selectivity, and specificity under mild conditions, and enzymatic catalysis has long been of great interest to chemical, pharmaceutical, and food industries,[181] though the use of enzymes for practical applications is often hindered by their low operational stability, difficult recovery, and lack of reusability under operational conditions.[182] It has been studied to immobilizing enzymes into the mesoporous materials, which can improve enzyme stability, facilitate separation and recycling, and maintain the catalytic activity and selectivity.[181-183] A step further would bring about enzymatic activities on the biocatalysts and thus obtain target products. Mesoporous zirconium organophosphonates with tunable mesopores, high surface area and large pore volume exhibited high adsorption capacity for lysozyme and papain, accompanied with rapid adsorption equilibrium speed.[177] The adsorption process involves physical surface interactions between the support matrix and the enzymes and can be driven by combined hydrogen bonding, electrostatic forces, and hydrophobic effects. For instance, the loading amount of lysozyme for hierarchically porous aluminum phosphonates could be easily adjusted by using phosphonic precurcors with different length of alkyl chains, finding that the longer the alkyl chain is, the higher loading capacity reaches.[151] But these physical interactions alone are not enough to keep the enzyme from desorbing from the support during catalysis. To improve the interactions, the metal phosphonates are tended to introduce additional groups such as carboxyl and amino, which could bind the enzymes tightly through covalent attachment involving amino acid residues of the enzymes. However, as to mesoporous metal phosphonates, the reports concerning these areas are still scarce, and it is suggested the following research to this uncultivated land.

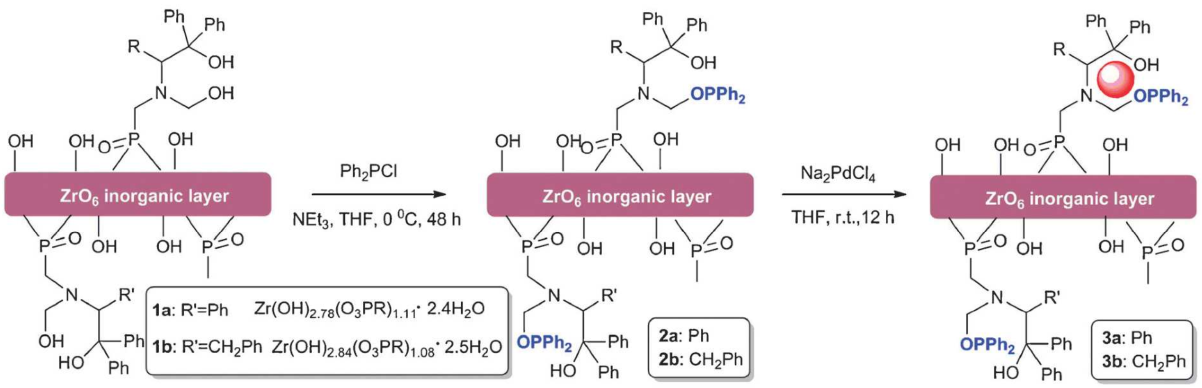

Fig. 8 Scheme of synthetic route to zirconium phosphonate-supported Pd catalysts.[175]

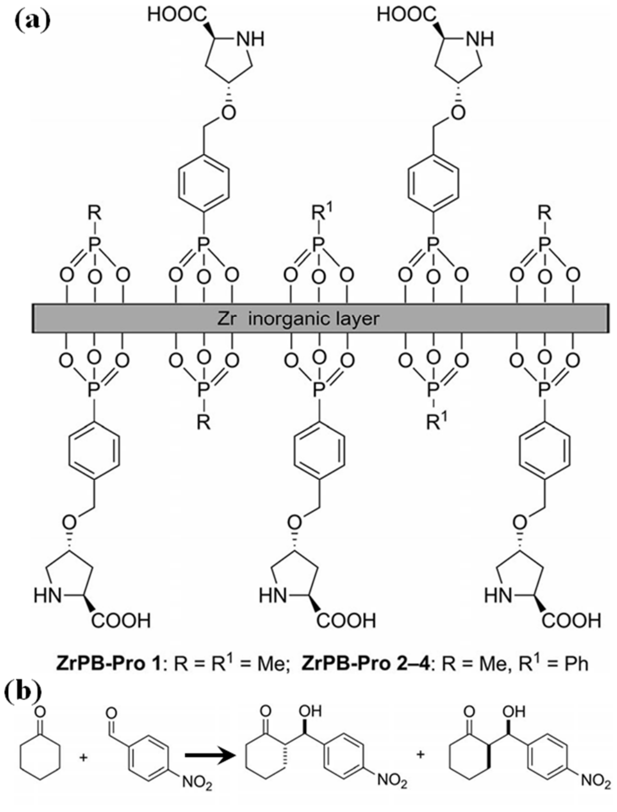

Fig. 9 Schematic arrangement of phosphonate groups on the layer of L-proline-functionalized zirconium phosphonates (a), and the corresponding catalytic aldol addition of cyclohexanone to p-nitrobenzaldehyde (b).[186,187]

3.2.3 Heterogeneous asymmetric catalysis. Asymmetric catalysis is of great importance for enantioselective synthesis of chemical compounds as their critical significance for pharmaceutical industry.[184] Chirality in metal phosphonates may offer new opportunities for applications beyond the traditional fields of chirality. Under this circumstance, inspired by the L-proline and its derivatives[185] widely used as organic catalysts for a wide range of enantioselective transformations, mesoporous metal phosphonates have been investigated as supports for immobilization of covalently linked chiral organic catalysts on the basis of the L-proline moiety. Zirconium phosphonates-supported L-proline prepared by using (4R)-4-(phosphonooxy)-L-proline were tested in the direct asymmetric aldol addition of cyclohexanones to p-nitrobenzaldehydes, showing high diastereoselectivity (*anti*/*syn* up to 94:6) and high enantiomeric excess (*ee*) up to 97% (**Fig. 9**).[186] A critical issue related to the unsatisfactory recoverability and reusability of the solid catalyst was due to the hydrolysis of phosphate ester bond that linked the L-proline to the host matrix. If a more stable phosphonate link was use to connect L-proline, no loss activity and reproducible anti/syn and *ee* values were achieved after six times cycles (**Fig. 9**).[187] Cinchonidine with the different arm lengths covalently immobilized onto the backbone of mesoporous zirconium phosphonate could be used for the preliminarily enantioselective addition of diethyl zinc to various aldehydes, which could be reused ten times without loss in the yield and enantiomeric excess.[188] Chiral salen Mn(III), exhibiting excellent catalytic activity and enantioselectivity for the asymmetric epoxidation of various unfunctional olefins,[189] were proven to be active chiral components grafted on porous metal phosphonates.[190] By grafting diamine or polyamine on zirconium phosphonates and subsequently axial coordination with chiral salen Mn(III) complexes, the coupled hybrids exhibited great activity and enantioselectivity in the asymmetric epoxidation of unfunctionalized olefins.[190] Especially, in the epoxidation of α-methylstyrene, both the conversion and *ee* could exceed 99%.

In spite of the catalytic activity and stability of the immobilized chiral units, the synthetic processes remain complicated due to the multiple steps such as prefunctionalization and immobilization. Amorphous zirconium phosphonates containing chiral functionalities such as 1,1'-bi-2-naphthol or 2,2'-bis(diphenylphosphino)-1,1'-binaphthyl were prepared and used as efficient heterogeneous catalysts in the stereoselective addition of diethylzinc to benzaldehyde, the aldol condensation and the hydrogenation of aromatic ketones and *β*-keto esters, showing high level of enantioselectivity.[191,192] A chiral borane of layered α-zirconium-N-(m-sulfophenyl)-L-valinephosphonate methanephosphonate has been used in the asymmetric Mukaiyama aldol reaction.[193] A porous, homochiral titanium phosphonate material based on a tripodal peptide scaffold was used as a heterogeneous reaction medium for the enantioselective hydration of styrene oxide.[194] Thereafter, the encapsulation of achiral salen Mn(III) within the homochiral mesoporous titanium phosphonate resulted in a new heterogeneous asymmetric catalyst for the formation of the *S* epoxide with high enantioselectivity and effective catalyst recovery.[195]

Direct graft of chiral moieties and introduction of phosphonate-based chiral groups have led to the generation of plentiful porous metal phosphonates. Noticeably, previous studies about chiral metal phosphonates for asymmetric catalysis are still prohibited by their inadequate mesoporosity and specific surface areas. Regarding the formation of a chiral superstructure, perhaps the most well–known and well–studied system is the formation of chiral mesoporous silica.[196-198] Chiral mesoporous siliceous materials can be created via using achiral or chiral surfactants.[199] Since surfactant-assisted synthesis methodology of mesoporous metal phosphonates actually refer to that of mesoporous siliceous materials, it can be imagined that chiral mesoporous phosphonates could be prepared in the presence of achiral surfactants or chiral phosphonate molecules and achiral surfactants, which can further enhance the asymmetric catalytic performance due to the maintenance of well–developed porosity on the level of fine pore system.

4. Potential precursors for metal phosphates

Considering the intimate relation between metal phosphonates and metal phosphates, mesoporous metal phosphonates may act as precursors in preparing metal phosphate counterparts with interesting structures and novel properties. The walls of metal phosphate molecular sieves are composed of oxygen atoms, which are larger than metal and phosphorus atoms. The character of the micropore, therefore, is fundamentally determined by the arrangement of the oxygen atoms and the elements incorporated in the framework. But the microporosity and the accessibility are confined to small molecules. Calcination of metal phosphonates were validated to be an efficient way to prepare mesoporous metal phosphates,[54 ,200-203] in which organic parts of the phosphonates released while leaving inorganic phosphate porous networks. Alternatively, calcination of mesoporous metal phosphonates in a proper region of temperature, usually around the decomposition of the hybrid framework composition, can bring "reproductive" mesoporous scaffolds of metal phosphate walls,[94] represent a feasible route to prepare mesoporous phosphates.

Nowadays, increasing demands have stimulated tremendous interest in alternative energy conversion and storage systems including metal–air batteries and fuel cell devices that are all intensively reminiscent of electrocatalytical processes, such as oxygen evolution reaction.[204,205] A key technical challenge for promoting the oxidative half–reaction that splits water to oxygen and protons is the discovery of efficient catalysts.[206] However, many of the most promising results have been provided by noble metals (compounds and oxides of iridium and ruthenium) and expensive graphene–based nanostructures.[207-211] Significantly, the voltage that is required to attain a given catalytic activity, referred as overpotential, limits the electrocatalytic efficiency. Along these lines, considerable attention is being focused on cobalt–based materials and the related compounds, particular interest was sparked by a series of recent reports by Nocera and co-workers on a cobalt phosphate materials containing oxy-hydroxide layers that operates as an electrocatalytic water-splitting catalyst.[212-219] The electrokinetic studies suggested a mechanism involving a rapid, one electron, one proton equilibrium between Co(III)–OH and Co(IV)–O in which a phosphate species was the proton acceptor, followed by a chemical turnover–limiting process involving oxygen–oxygen bond coupling.[213-215] Interestingly, the self-repair peculiarity of the phosphates ensured the long-term stability of the catalyst systems. Nanostructured $Co(PO_3)_2$ materials derived from thermal processing of a molecular precursor could be decorated on nickel electrode and further evaluated as an anode for water oxidation electrocatalysis in nearly neutral phosphate-buffered water (**Fig. 10**).[219] Catalytic onset occurred at an overpotential of about 310 mV, which was 100 mV lower than that observed for Co_3O_4 nanoparticles with a comparable surface area and the cobalt phosphate thin film catalyst (CoPi) [212] under identical conditions. A per-metal turnover frequency (TOF) of 0.10–0.21 s^{-1} was observed at overpotential of 440 mV, which was comparable to the highest rate reported for a first-row metal heterogeneous catalyst. Spectroscopic studies revealed that the surface of the $Co(PO_3)_2$-based electrocatalyst underwent restructuring during electrocatalysis, resulting in bound CoO_x species supported by the underlying $Co(PO_3)_2$ structure. The anion in the catalyst material, as well as the nature of the interaction between the catalytic, surface-bound species and the support material appeared to play roles in water oxidation catalysis. Investigations of cobalt-based inorganic materials with a range of anions should help to develop structure–function relations and point the way to more efficient catalysts.

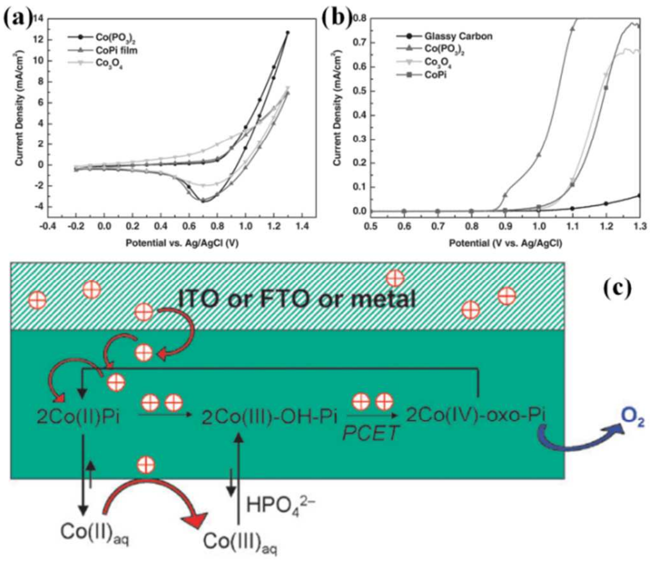

Fig. 10 (a) Comparison of CVs of three different materials at a scan rate of 100 mV/s (all of the electrocatalysts were deposited on Ni foam), and (b) LSV of the catalysts in comparison are shown on the right. Catalytic onset of the nanostructured $Co(PO_3)_2$ catalyst at a significantly lower potential was observed. The nonlinearity of the catalytic current at high overpotentials was due to large changes in the electrode area arising from vigorous bubble formation.[219] (c) A working model for the Co–phosphate oxygen-evolving.[214]

One should keep in mind that the cobalt phosphates are usually operated in neutral solutions and exhibit instability in strongly acidic and basic condition, making them promising in natural environments. An electrolyte environment that has good proton–accepting properties is favourable for sustained catalyst activity at appreciable current density, and the phosphate electrolyte is an efficient proton carrier and can preserve a stable local pH environment for high catalytic activity.[220] Additionally, it functions as an acceptor of the protons furnished from water oxidation and participates in the proton–coupled electron transfer (PCET) activation of oxygen (**Fig. 10**). Other alternative electrolytes that are able to support catalysis are desirable as long they have sufficient proton-accepting capacity in the pH region of interest and are stable under the conditions of catalysis.

Mesoporous zirconium phosphates with large surface area and thermally stable acidity could be synthesized by calcination of mesoporous zirconium phoshonates.[221] The acidity was confirmed to be strong Lewis and Brönsted acid sites.[222,223] These mesoporous zirconium phosphate materials with high acid density showed excellent catalytic activity in biodiesel reaction for the effective conversion of the long chain fatty acids to their respective methyl esters.[223] Large pore size that favoured the diffusion of large organic molecules contributed to the enhancement of catalytic ability. High catalytic activity could be attributed to the large surface area and the presence of large number of acidic sites located at the surface of the materials. The catalysts showed negligible loss of activity after five repetitive cycles, suggesting high chemical stability and reusability of the mesoporous zirconium oxophosphate framework. The thermal stability of acidic sites for the resulting metal phosphates would suit some harsh applications such as dehydrogenation of alkanes to alkenes that needs high temperature process.[224,225]

Crystalline metal phosphate catalysts have already played important roles in practical industrial production. But there are still little studies on the metal phosphonate–derived phosphates for catalysis. The consumption of organic functionalities and the escape of volatile components including CO_2 and H_2O during the heat treatment under aerobic conditions may create novel porosity as compared from conventional techniques to synthesize metal phosphates. Apart from the above mentioned electrocatalysis, esterification and dehydrogenation reaction, metal phosphate semiconductors-mediated photocatalyis[226,227] can be imagined. Reversely, under anaerobic conditions, the decomposition of homogeneous organics can lead to the formation of carbon networks, on which the phosphate species are highly dispersed.[228,229]

5. Conclusions and Outlook

This review has highlighted the progress of mesoporous metal phosphonates for heterogeneous catalysis, aiming at shedding light on the origins of activity and providing basic principles for designing high-efficiency metal phosphonate catalysts. Metal phosphonates hybrid materials with combined peculiarities of organic and inorganic components have become a burgeoning member of the heterogeneous catalysts. Through ligand extension, template–free self–assembly, and supermolecular template induction strategies, reasonable introduction of mesoporosity into the metal phosphonate frameworks can hugely improve the catalytic activity and influence the selectivity and reaction processes. The relatively strong bonding between phosphonics and metal joints ensures the network stability and homogeneous distribution of catalytic sites, and thereby, mesoporous metal phosphonates have been shown to outperform other porous materials in some catalytic areas. The metal nodes can perform as Lewis acid sites and redox centers, holding promise for the reactions involving activation of carbonyls and molecular oxygen, hydrogenation, and oxidation. The organophosphonate groups show inherent functionalities and capacities for post–modification including sulfonation, bromination, grafting and supporting. As a consequence, the rational choice and ingenious functionalization can make mesoporous metal phosphonates promising in the fields of biofuel and drug synthesis, chiral catalysis, and environment and energy relevant catalysis. Bearing in mind the similarities to metal phosphates, preformed mesoporous metal phosphonates can be used as sources for phosphate counterparts with novel physicochemical properties, which is reminiscent of MOF–derived materials.[230,231] In that way, further development based on this new and versatile synthesis method is very interesting and necessary; for example, cobalt phosphates as alternative electrode materials exhibited high oxygen evolution activity.[232] To sum up the research advances and efforts, great potential and huge challenges coexist in this field. Catalysis based on mesoporous metal phosphonate materials is still in its early research stage.

Heterogeneous catalysis, not confined to metal phosphonates, is indeed an extremely host–guest interaction process occurring at the interfaces, and many relevant fundamental aspects are not fully understood. It is urgent to clearly unravel the catalytic mechanisms, which is regarded as a prerequisite to guide the design of efficient hybrid heterogeneous materials. Good predictive power arises from in–depth insights into the catalytic mechanism and the correlation between materials properties and performance. A combination of in situ experimental analysis, isotope labelling, theoretical investigation, nanoscale probing, atomic scale modelling would be valuable to get such insights.

Besides the requirement of fundamental mechanistic study, it is of paramount importance to make efforts for the enhancement of the thermal and hydrothermal stability of mesoporous metal phosphonate materials. Solution to this issue should resort to the crystalline mesopore wall. This is a regardful factor in practical catalytic applications. The mesostructure with crystalline pore walls has long been a hot topic. Noticeably, the unpredictable ligating mode of phosphonate groups would facilitate the formation of networks with low degrees of order. On the consideration that crystallization usually accompanies the collapse of mesostructures, the interactions between surfactants and hybrid species or the roles of surfactants should be of more prominence. If the crystallization can happen at a condition that surfactant micelles are immobilized inside the mesostructured scaffolds, confined crystallization on hybrid mesopore walls may come into being. And the use of ionic block copolymers with amine headgroups is expected. Adjusting the synthetic parameters such as temperature and time could realize the control of mesophases.[232-236] Reducing the reaction rates of metallic precursors represents another choice to contribute to the formation of well–structured mesoporosity. Alleviation by organic reagents, low temperature and supercritical conditions would possibly aid in the design of mesoporous metal phosphonates with crystalline walls. On the other hand, the crystalline metal phosphonates are usually of difficultly determined structures. Exploration of high–throughput hydrothermal or solvothermal techniques and advances in powder X–ray diffraction modelling and refinement will significantly increase the number of structurally characterized crystalline metal phosphonates, and it will be exciting to watch this field as it develops.

The increasing interest in the field of mesoporous metal phosphonate–based heterogeneous catalysis will be amplified. In modern times, the solid state chemistry, organic synthesis, and electronic techniques have reached a high level of sophistication. It is reasonable to imagine that metal phosphonates of desired mesostructures and catalytic functionalities can be designed at the molecular scale in the future. These advances must be made in conjunction with analytic and resolved studies that will further elucidate the true value of hybrid materials. Undoubtedly, realizing the fantastic promise held by mesoporous metal phosphonates requires ongoing research attention and efforts from various disciplines to address the formidable challenges. The lack of industrial applications dose not signify that the interest in metal phosphonates has been prohibited; on the contrary, the huge amount of efforts has contributed to identify the potentialities and the intrinsic limitations, stimulating the exploration of novel methodologies that point to new materials with enhanced physicochemical and catalytic properties.

Acknowledgements

This work was supported by the National Natural Science Foundation of China (21421001), the Program for Innovative Research Team in University (IRT13022), the 111 project (B12015), and the Ph.D. Candidate Research Innovation Fund of Nankai University.

Notes and references

[a] Key Laboratory of Advanced Energy Materials Chemistry (Ministry of Education), Collaborative Innovation Center of Chemical Science and Engineering (Tianjin), College of Chemistry, Nankai University, Tianjin 300071, China. E-mail: zyyuan@nankai.edu.cn.
[b] School of Chemical Engineering and Technology, Hebei University of Technology, Tianjin 300130, China.

1. L. Yin and J. Liebscher, *Chem. Rev.*, 2007, **107**, 133–173.
2. W. M. Dai, Y. Li, Y. Zhang, C. Yue and J. Wu, *Chem.–Eur. J.*, 2008, **14**, 5538–5554.
3. S. Kotha and K. Mandal, *Chem.–Asian J.*, 2009, **4**, 354–362.
4. S.MacQuarrie, J. H. Horton, J. Barnes, K. McEleney, H. P. Loock and C. M. Crudden, *Angew. Chem. Int. Ed.*, 2008, **47**, 3279–3282.
5. Y. Jia, M. Bios-Choussy and J. Zhu, *Angew. Chem. Int. Ed.*, 2008, **47**, 4167–4172.
6. R. A. Sheldon, *Chem. Commun.*, 2008, 3352–3365.
7. S. Shylesh, V. Schünemann and W. R. Thiel, *Angew. Chem., Int. Ed.*, 2010, **49**, 3428–3459.
8. A. Schätz, O. Reiser and W. J. Stark, *Chem.–Eur. J.*, 2010, **16**, 8950–8967.
9. Z. Luo, Q. Zhang, Y. Oderaotoshi and D. P. Curran, *Science*, 2001, **291**, 1766–1769.
10. N. N. Tušar, S. Jank and R. Gläser, *ChemCatChem*, 2011, **2**, 254–269.
11. M. N. Timofeevaa, V. N. Panchenkoa, Z. Hasanc and S. H. Jhung, *Appl. Catal. A*, 2013, **45**, 71–85.
12. A. Bhaumik and S. Inagaki, *J. Am. Chem. Soc.*, 2001, **4**, 691–696.
13. L. Liu, Q. F. Deng, Y. P. Liu, T. Z. Ren and Z. Y. Yuan, *Catal. Commun.*, 2011, **1**, 81–85.
14. L. Liu, Q. F. Deng, B. Agula, X. Zhao, T. Z. Ren and Z. Y. Yuan, *Chem. Commun.*, 2011, **47**, 8334–8336.
15. W. Kicińskia, M. Szalaa, M. Bystrzejewski, *Carbon*, 2014, **68**, 1–32.
16. H. W. Liang, J. W. Liu, H. S. Qian and S. H. Yu, *Acc. Chem. Res.*, 2013, **46**, 1450–1461.
17. Y. P. Zhu, T. Z. Ren, Y. P. Liu and Z. Y. Yuan, *RSC Adv.*, 2014, **4**, 31754–31758.
18. I. E. Wachs, *Catal. Today*, 2005, 100, 79–94.
19. Y. P. Zhu, T. Z. Ren, T. Y. Ma, and Z. Y. Yuan, *Int. J. Photoenergy*, 2014, **2014**, 498540.
20. Y. P. Zhu, M. Li, Y. L. Liu, T. Z. Ren and Z. Y. Yuan, *J. Phys. Chem. C*, 2014, **118**, 10963–10971.
21. Y. P. Zhu, J. Li, T. Y. Ma, Y. P. Liu, G. H. Du and Z. Y. Yuan, *J. Mater. Chem. A*, 2014, **2**, 1093–1101.
22. Z. Y. Yuan and B. L. Su, *J. Mater. Chem.*, 2006, **16**, 663–677.
23. X. Y. Yang, A. Léonard, A. Lemaire, G. Tian and B. L. Su, *Chem. Commun.*, 2011, **47**, 2763–2786.
24. D. Chandra, N. Mukherjee, A. Mondal and A. Bhaumik, *J. Phys. Chem. C*, 2008, **112**, 8668–8674.
25. G. K. H. Shimizu, R. Vaidhyanathan and J. M. Taylor, *Chem. Soc. Rev.*, 2009, 38, 1430–1449.
26. Y. P. Zhu, T. Y. Ma, T. Z. Ren and Z. Y. Yuan, *ACS Appl. Mater. Interfaces*, 2014, **6**, 16344−16351.
27. H. Li, T. Y. Ma, D. M. Kong and Z. Y. Yuan, *Analyst*, 2013, *138*, 1084–1090.
28. M. S. Bhattacharyya, P. Hiwale, M. Piras, L. Medda, D. Steri, M. Piludu, A. Salis and M. Monduzzi, *J. Phys. Chem. C*, 2010, **114**, 19928–19934.
29. Z. Zhou, R. N. K. Taylor, S. Kullmann, H. Bao and M. Hartmann, *Adv. Mater.*, 2011, **23**, 2627–2632.
30. A. Clearfield, C. V. K. Sharma and B. Zhang, *Chem. Mater.*, 2001, **13**, 3099–3112.
31. K. J. Gagnon, H. P. Perry and A. Clearfield, *Chem. Rev.*, 2012, **112**, 1034–1054.
32. L. Yang, Q. Zhu, S. Guo, B. Qian, C. Xia and H. Huang, *Chem. Eur. J.*, 2010, **16**, 1638–1645.
33. V. Lykourinou, Y. Chen , X. S. Wang, L. Meng, T. Hoang, L. J. Ming, R. L. Musselman and S. Ma, *J. Am. Chem. Soc.*, 2011, **133**, 10382–10385.
34. Y. P. Zhu, T. Z. Ren and Z. Y. Yuan, *New J. Chem.*, 2014, **38**, 1905–1922.
35. Y. P. Zhu, T. Y. Ma, Y. L. Liu, T. Z. Ren and Z. Y. Yuan, *Inorg. Chem. Front.*, 2014, **1**, 360–383.
36. F. Q. Wang, W. H. Mu, X. J. Zheng, L. C. Li, D. C. Fang and L. P. Jin, *Inorg. Chem.*, 2008, **47**, 5225–5233
37. A. G. W. Foy, O. Lebel and A. J. Matzger, *J. Am. Chem. Soc.*, 2007, **129**, 15740–15741.
38. T. Y. Ma and Z. Y. Yuan, *ChemSusChem*, 2011, **4**, 140–1419.
39. T. Y. Ma, H. Li, A. N. Tang and Z. Y. Yuan, *Small*, 2011, **4**, 1407–1417.
40. C. T. Kresge, M. E. Leonowicz, W. J. Roth, J. C. Vartuli and J. S. Beck, *Nature*, 1992, **359**, 710–712.
41. Y. Wan and D. Zhao, *Chem. Rev.*, 2007, **107**, 2821–2860.

42. G. Alberti, R. Vivani, F. Marmottini and P. Zappelli, *J. Porous Mater.*, 1998, **5**, 205–220.
43. A. Clearfield, *Chem. Mater.*, 1998, **10**, 2801–2810.
44. M. V. Vasylyev, E. J. Wachtel, R. Popovitz-Biro and R. Neumann, *Chem. Eur. J.*, 2006, **12**, 3507–3514.
45. M. Vasylyev and R. Neumann, *Chem. Mater.*, 2006, **18**, 2781–2783.
46. S. Konar, J. Zon, A. V. Prosvirin, K. R. Dunbar and A. Clearfield, *Inorg. Chem.*, 2007, **26**, 5229–5236.
47. T. Y. Ma, X. J. Zhang and Z. Y. Yuan, *J. Mater. Sci.*, 2009, **44**, 6775–6785.
48. X. J. Zhang, T. Y. Ma and Z. Y. Yuan, *Eur. J. Inorg. Chem.*, 2008, 2721–2726.
49. T. Z. Ren, X. H. Zhu, T. Y. Ma, Z. Y. Yuan, *Adsorption Sci. Technol.*, 2013, **31**, 535–548.
50. X. J. Zhang, T. Y. Ma, Z. Y. Yuan, *Chem. Lett.*, 2008, **37**, 746–747.
51. T. Kimura, *Chem. Mater.*, 2005, **17**, 5521–5528.
52. T. Kimura, *Chem. Mater.*, 2003, **15**, 3742–3744.
53. T. Kimura, *Chem. Mater.*, 2005, **17**, 337–344.
54. T. Y. Ma, X. Z. Lin and Z. Y. Yuan, *Chem.–Eur. J.*, 2010, **16**, 8487–8494.
55. T. Kimura, *J. Nanosci. Nanotechnol.,* 2013, **13**, 2461–2470.
56. A. Clearfield, *Prog. Inorg. Chem.*, 1998, **47**, 371–510.
57. A. Vioux, J. le Bideau, P. H. Mutin and D. Leclercq, *Top. Curr. Chem.*, 2004, **232**, 145–174.
58. G. Alberti, U. Costantino, F. Marmottini, R. Vivani and P. Zappelli, *Angew. Chem.*, 1993, **105**, 1396–1402.
59. Q. Yue, J. Yang, G. H. Li, G. D. Li and J. S. Chen, *Inorg. Chem.*, 2006, **45**, 4431–4439.
60. O. M. Yaghi, H. Li, C. Davis, D. Richardson and T. L. Groy, *Acc. Chem. Res.*, 1998, **31**, 474–484.
61. X. S. Wang, S. Q. Ma, D. F. Sun, S. Parkin and H. C. Zhou, *J. Am. Chem. Soc.*, 2006, **128**, 16474–16475.
62. Z. H. Nie, A. Petukhova and E. Kumacheva, *Nat. Nanotechnol.*, 2010, **5**, 15–25.
63. G. Alberti, F. Marmottini, R. Vivani and P. Zappelli, *J. Porous Mater.*, 1998, **5**, 205–220.
64. Y. P. Zhu, Y. L. Liu, T. Z. Ren and Z. Y. Yuan, *RSC Adv.*, 2014, **4**, 16018–16021.
65. L. Li, S. L. Xiang, S. Q. Cao, J. Y. Zhang, G. F. Ouyang, L. P. Chen and C. Y. Su, *Nat. Commun.*, 2013, **4**, 1774.
66. D. Zacher, R. Schmid, C. Woll and R. A. Fischer, *Angew. Chem., Int. Ed.*, 2011, **50**, 176–199.
67. C. Sanchez, P. Belleville, M. Popall and L. Nicole, *Chem. Soc. Rev.*, 2011, **40**, 696–753.
68. Z. Y. Yuan, A. Vantomme, A. Leonard and B. L. Su, *Chem. Commun.*, 2003, 1558–1559.
69. Z. Y. Yuan, T. Z. Ren, A. Vantomme and B. L. Su, *Chem. Mater.*, 2004, 16, 5096–5106.
70. Y. Li, X. Y. Yang, G. Tian, A. Vantomme, J. G. Yu, G. V. Tendeloo and B. L. Su, *Chem. Mater.*, 2010, **22**, 3251–3258.
71. Y. H. Deng, J. Wei, Z. K. Sun and D. Y. Zhao, *Chem. Soc. Rev.*, 2013, 42, 4054–4070.
72. W. Li, Q. Yue, Y. H. Deng and D. Y. Zhao, *Adv. Mater.*, 2013, **25**, 5129–5152.
73. G. J. de A. A. Soler-Illia and C. Sanchez, *New J. Chem.*, 2000, **24**, 130 493–499.
74. G. J. de A. A. Soler-Illia, E. Scolan, A. Louis, P. A. Albouy and C. Sanchez, *New J. Chem.*, 2001, **25**, 156–165.
75. S. Cabrera, J. E. Haskouri, S. Mendioroz, C. Guillem, J. Latorre, A. Beltrán, D. Beltrán, M. D. Marcos and P. Amorós, *Chem. Commun.*, 1999, 1679.
76. J. E. Haskouri, C. Guillem, J. Latorre, A. Beltrán, D. Beltrán and P. Amorós, *Eur. J. Inorg. Chem.*, 2004, 1804–1807.
77. J. E. Haskouri, C. Guillem, J. Latorre, A. Beltrán, D. Beltrán and P. Amorós, *Chem. Mater.*, 2004, **16**, 4359–4372.
78. T. Y. Ma, H. Li, Q. F. Deng, L. Liu, T. Z. Ren and Z. Y. Yuan, *Chem. Mater.*, 2012, **24**, 2253–2255.
79. S. Cao, G. Gody, W. Zhao, S. Perrier, X. Y. Peng, C. Ducati, D. Y. Zhao and A. K. Cheetham, *Chem. Sci.*, 2013, **4**, 3573–3577.
80. T. Kimura, D. Nakashima and N. Miyamoto, *Chem. Lett.*, 2009, **38**, 916–917.
81. B. C. Garcia, M. Kamperman, R. Ulrich, A. Jain, S. M. Gruner and U. Wiesner, *Chem. Mater.*, 2009, **21**, 5397–5405.
82. S. A. El-Safty, F. Mizukami and T. Hanaoka, *J. Phys. Chem. B*, 2005, **20**, 9255–9264.
83. S. A. El-Safty, T. Hanaoka and F. Mizukami, *Chem. Mater.*, 2005, **17**, 3137–3145.
84. T. Kimura and K. Kato, *New J. Chem.*, 2007, **31**, 1488–1492.
85. T. Kimura and K. Kato, *Micropor. Mesopor. Mater.*, 2007, **101**, 207–213.
86. T. Kimura and K. Kato, *J. Mater. Chem.*, 2007, **17**, 559–566.
87. T. Kimura and Y. Yamauchi, *Chem. Asian J.*, 2013, **8**, 160–167.
88. T. Kimura, *Chem. Asian J.*, 2011, **6**, 3236–3242.
89. T. Kimura, N. Suzuki, P. Gupta and Y. Yamauchi, *Dalton Trans.*, 2010, **39**, 5139–5144.
90. T. Kimura, K. Katoa and Y. Yamauchi, *Chem. Commun.*, 2009, 4938–4940.
91. T. Kimura and Y. Yamauchi, *Langmuir*, 2012, **28**, 12901−12908.
92. G. Guerrero, J. G. Alauzun, M. Granier, D. Laurencin and P. H. Mutin, *Dalton Trans.*, 2013, **42**, 12569–12585.
93. T. Y. Ma, X. J. Zhang and Z. Y. Yuan, *Micropor. Mesopor. Mater.*, 2009, **123**, 234–242.
94. T. Y. Ma, X. Z. Lin and Z. Y. Yuan, *J. Mater. Chem.*, 2010, **20**, 7406–7415.
95. G. S. Shao, X. J. Zhang and Z. Y. Yuan, *Appl. Catal. B*, 2008, **82**, 208–218.
96. T. Y. Ma, X. J. Zhang, G. S. Shao, J. L. Cao and Z. Y. Yuan, *J. Phys. Chem. C*, 2008, **112**, 3090–3096.
97. M. Pramanik, A. K. Patra and A. Bhaumik, *Dalton Trans.*, 2013, **42**, 5140–5149.
98. H. Imahori, T. Umeyama and S. Ito, *Acc. Chem. Res.*, 2009, **42**, 1809–1818.
99. T. Y. Ma, Y. S. Wei, T. Z. Ren, L. Liu, Q. Guo and Z. Y. Yuan, *ACS Appl. Mater. Interfaces*, 2010, **2**, 3563–3571.
100. T. P. Brewster, S. J. Konezny, S. W. Sheehan, L. A. Martini, C. A. Schmuttenmaer, V. S. Batista and R. H. Crabtree, *Inorg. Chem.*, 2013, **52**, 6752–6764.
101. R. Luschtinetz, J. Frenzel, T. Milek and G. Seifert, *J. Phys. Chem. C*, 2009, **113**, 5730–5740.

102. M. Renz, T. Blasco, A. Corma, V. Fornés, R. Jensen and L. Nemeth, *Chem.–Eur. J.*, 2002, **8**, 4708–4717.

103. A. Corma, L. Nemeth, M. Renz and S. Valencia, *Nature*, 2001, **412**, 423–425.

104. A. Corma, V. Fornés, S. Iborra, M. Mifsud and M. Renz, *J. Catal.*, 2004, **221**, 67–76.

105. S. Kirumakki, S. Samarajeewa, R. Harwell, A. Mukherjee, R. H. Herberb and A. Clearfield, *Chem. Commun.*, 2008, 5556–5558.

106. A. Dutta, M. Pramanik, A. K. Patra, M. Nandi, H. Uyama and A. Bhaumik, *Chem. Commun.*, 2012, **48**, 6738–6740.

107. A. Fassihi, K. Mahnam, B. Moeinifard, M. Bahmanziari, H. S. Aliabadi, A. Zarghi, R. Sabet, M. Salimi and M. Mansourian, *Med. Chem. Res.*, 2012, **21**, 2749–2761.

108. M. Pramanik and A. Bhaumik, *J. Mater. Chem. A*, 2013, **1**, 11210–11220.

109. M. Pramanik and A. Bhaumik, *ChemCatChem*, 2014, **6**, 2577–2586.

110. A. Dutta, J. Mondal, A. K. Patra and A. Bhaumik, *Chem.–Eur. J.*, 2012, **18**, 13372–13378.

111. M. Kouzu, S. Yamanaka, J. Hidaka and M. Tsunomori, *Appl. Catal. A*, 2009, **355**, 94–99.

1112. A. L. Cardoso, S. C. G. Neves and M. J. Silva, *Energy Fuels*, 2009, **23**, 1718–1722.

113. M. Pramanik and A. Bhaumik, *Chem.–Eur. J.*, 2013, **19**, 8507–8514.

114. J. El Haskouri, A. Moragues, A. Beltrán, S. Murcia-Mascarós, F. Plazaola, E. Legarra, A. Mauri-Aucejo, M. Brotons-Gisbert, J. F. Sánchez-Royo, D. Beltrán and P. Amorós, *Micropor. Mesopor. Mater.*, 2014, **187**, 14–22.

115. N. K. Mal, A. Bhaumik, M. Matsukata and M. Fujiwara, *Ind. Eng. Chem. Res.*, 2006, **45**, 7748–7751.

116. A. Dutta, A. K. Patra, H. Uyama and A. Bhaumik, *ACS Appl. Mater. Interfaces*, 2013, **5**, 9913−9917.

117. M. Blosi, S. Albonetti, A. L. Costa, N. Sangiorgi and A. Sanson, *Chem. Eng. J.*, 2013, **215**, 616–625.

118. Y. Du, H. L. Chen, R. Z. Chen and N. P. Xu, *Appl. Catal. A*, 2004, **277**, 259–264

119. A. Dutta, A. K. Patra and A. Bhaumik, *Micropor. Mesopor. Mater.*, 2012, **155**, 208–214.

120. Y. Liu, Y. Fan, Y. Yuan, Y. Chen, F. Cheng and S. C. Jiang, *J. Mater. Chem.*, 2012, **22**, 21173–21182.

121. Y. P. Zhu, T. Z. Ren and Z. Y. Yuan, *Nanoscale*, 2014, **6**, 11395–11402.

122. J. Fernandez, P. Muruthamuthu, A. Renken and J. Kiwi, *Appl. Catal., B*, 2004, **49**, 207–215.

123. Y. P. Zhu, Y. L. Liu, T. Z. Ren and Z. Y. Yuan, *Nanoscale*, 2014, **6**, 6627–6636.

124. M. Pramanik, M. Nandi, H. Uyama and A. Bhaumik, *Catal. Sci. Technol.*, 2012, **2**, 613–620.

125. G. P. Anipsitakis and D. D. Dionysiou, *Environ. Sci. Technol.*, 2004, **38**, 3705–3712.

126. M. Boronat, A. Corma, M. Renz, G. Sastre and P. M. Viruela, *Chem.–Eur. J.*, 2005, **11**, 6905–6915.

127. N. Pal, M. Pramanik, Md. M. Seikh and A. Bhaumik, *J. Magn. Magn. Mater.*, 2014, **363**, 210–216.

128. M. Vasylyev and R. Neumann, *Chem. Mater.*, 2006, **18**, 2781–2783.

129. V. M. Rakića, R. V. Hercigonja and V. T. Dondur, *Micropor. Mesopor. Mater.*, 1999, **27**, 27–39.

130. P. E. Cürdaneli1 and S. Özkar, *Micropor. Mesopor. Mater.*, 2014, **196**, 51–58.

131. T. Y. Ma, X. Z. Lin, X. J. Zhang and Z. Y. Yuan, *Nanoscale*, 2011, **3**, 1690–1696.

132. X. Z. Lin and Z. Y. Yuan, *Eur. J. Inorg. Chem.*, 2012, 2661–2664.

133. X. J. Zhang, T. Y. Ma and Z. Y. Yuan, *J. Mater. Chem.*, 2008, **18**, 2003–2010.

134. T. Y. Ma, L. Liu, Q. F. Deng, X. Z. Lin and Z. Y. Yuan, *Chem. Commun.*, 2011, **47**, 6015–6017.

135. R. Q. Zeng, X. K. Fu, C. B. Gong, Y. Sui, X. B. Ma and X. B. Yang, *J. Mol. Catal. A*, 2005, **229**, 1–5.

136. J. L. Song, Z. F. Zhang, S. Q. Hu, T. B. Wu, T. Jiang and B. X. Han, *Green Chem.*, 2009, **11**, 1031–1036.

137. O. V. Zalomaeva, A. M. Chibiryaev, K. A. Kovalenko, O. A. Kholdeeva, B. S. Balzhinimaev, V. P. Fedin, *J. Catal.*, 2013, **298**, 179–185.

138. J. Kim, S. N. Kim, H. G. Jang, G. Seo and W.S. Ahn, *Appl. Catal. A*, 2013, **453**, 175–180.

139. Y. Xie, T. T. Wang, X. H. Liu, K. Zou and W. Q. Deng, *Nat. Commun.*, 2013, **4**,1960.

140. X. Z. Lin, Z. Z. Yang, L. N. He and Z. Y. Yuan, *Green. Chem.*, 2015, **17**， 795–798.

141. T. Y. Ma and S. Z. Qiao, *ACS Catal.*, 2014, **4**, 3847−3855.

142. Z. Wang, J. M. Heising and A. Clearfield, *J. Am. Chem. Soc.*, 2003, **125**, 10375–10383.

143. N. K. Mal, M. Fujiwara and A. Bhaumik, *J. Non–Cryst. Solids*, 2007, **353**, 4116–4120.

144. M. Pramanik, M. Nandi, H. Uyama and A. Bhaumik, *Green Chem.*, 2012, **14**, 2273–2281.

145. M. G. Goesten, J. Juan-Alcañiz, E. V. Ramos-Fernandez, K. B. S. S. Gupta, E. Stavitski, H. van Bekkum, J.Gascon and F. Kapteijn, *J. Catal.*, 2011, **281**, 177–187.

146. T. Y. Ma and Z. Y. Yuan, *Chem. Commun.*, 2010, **46**, 2325–2327.

147. Mi. G. Mazzotta, D. Gupta, B. Saha, A. K. Patra, A. Bhaumik and M. M. Abu-Omar, *ChemSusChem*, 2014, **7**, 2342–2350.

148. S. K. Das, M. K. Bhunia, A. K. Sinh and A. Bhaumik, *ACS Catal.*, 2011, **1**, 493–501.

149. D. Lanari, F. Montanari, F. Marmottini, O. Piermatti, M. Orrù and L. Vaccaro, *J. Catal.*, 2011, **277**, 80–87.

150. T. Y. Ma, X. J. Zhang and Z. Y. Yuan, *J. Phys. Chem. C*, 2009, 113, 12854–12862.

151. K. Inumaru, T. Ishihara, Y. Kamiya, T. Okuhara and S. Yamanaka, *Angew. Chem. Int. Ed.*, 2007, **46**, 7625 –7628.

152. X. Z. Lin, T. Z. Ren, Z. Y. Yuan, *Catal. Sci. Technol.*, 2015, **5**, 1485–1494.

153. M. G. Goesten, J. Juan-Alcañiz, E. V. Ramos-Fernandez, K. B. S. S. Gupta, E. Stavitski, H. van Bekkum, J. Gascon and F. Kapteijn, *J. Catal.*, 2011, **281**, 177–187.

154. S. Mo, X. Q. Zhao, Y. Chen, L. Liu, R. Wang and Q. H. Xu, *Mater. Chem. Phys.*, 2013, **140**, 228–235.

155. J. V. Coelho, M. S. Guedes, R. G. Prado, J. Tronto, J. D. Ardissonc, M. C. Pereirad and L. C. A. Oliveir, *Appl. Catal., B*, 2014, **144**, 792–799.
155. S. H. Tian, Y. T. Yu, D. S. Chen, X. Chen and Y. Xiong, *Chem. Eng. J.*, 2011, **169**, 31–37.
157. L. Q. Guo, F. Chen, X. Q. Fan, W. D. Cai and J. L. Zhang, *Appl. Catal. B*, 2010, **96**, 162–168.
158. Y. P. Zhu, T. Z. Ren and Z. Y. Yuan, *RSC adv.*, 2015, **5**, 7628–7636.
159. H. Byrd, A. Clearfield, D. Poojary, K. P. Reis and M. E. Thompson, *Chem. Mater.*, 1996, **8**, 2239–2246.
160. X. B. Ma and X. K. Fu, *J. Mol. Catal. A*, 2004, **208**, 129–133.
161. H. P. Perry, J. Law, J. Zon and A. Clearfield, *Micropor. Mesopor. Mater.*, 2012, **149**, 172–180.
162. X. Y. Liu, A. Q. Wang, X. F. Yang, T. Zhang, C. Y. Mou, D. S. Su and J. Li, *Chem. Mater.*, 2009, **21**, 410–418.
163. H. L. Yu, X. Jun, J. C. Zong, L. Zhen, T. Feng, R. Z. Li, F. W. Hai, P. Hu, J. Z. Hui and G. Y. Hua, *Nat. Commun.*, 2013, **4**, 2500.
164. K. Sakai and H. Ozawa, *Coord. Chem. Rev.*, 2007, **251**, 2753–2766.
165. H. C. Qin, W. Y. Li, Y. J. Xia and T. He, *ACS Appl. Mater. Interfaces*, 2011, **3**, 3152−3156.
166. J. R. Ran, J. Zhang, J. G. Yu, M. Jaroniec and S. Z. Qiao, *Chem. Soc. Rev.*, 2014, **43**,7787−7812.
167. Y. P. Zhu, T. Y. Ma, T. Z. Ren, J. Li, G. H. Du and Z. Y. Yuan, *Appl. Catal. B*, 1014, **156−157**, 44−52.
168. J. L. Cao, Y. Wang, X. L. Yu, S. R. Wang, S. H. Wu and Z. Y. Yuan, *Appl. Catal., B*, 2008, 79, 26−34.
169. M. F. Luo, J. M. Ma, J. Q. Lu, Y. P. Song and Y. J. Wang, *J. Catal.*, 2007, **246**, 52–59.
170. T. Y. Ma and Z. Y. Yuan, *Dalton Trans.*, 2010, **39**, 9570–9578.
171. X. B. Ma, J. Liu, L. S. Xiao, R. Chen, J. Q. Zhou and X. K. Fu, *J. Mater. Chem.*, 2009, **19**, 1098–1104.
172. T. T. Chen, X. B. Ma, X. J. Wang, Q. Wang, J. Q. Zhou and Q. Tang, *Dalton Trans*., 2011, **40**, 3325–3335.
173. X. J. Wang, X. B. Ma, T. T. Chen, X. L. Qin and Q. Tang, *Catal. Commun.*, 2011, **12**, 583–588.
174. D. E. Bergbreiter, J. H. Tian and C. Hongfa, *Chem. Rev.*, 2009, **109**, 530–582.
175. Y. Y. Ma, X. B. Ma, Q. Wang and J. Q. Zhou, *Catal. Sci. Technol.*, 2012, **2**, 1879–1885.
176. S. Hudson, J. Cooney and E. Magner, *Angew. Chem., Int. Ed.*, 2008, **47**, 8582–8594.
177. X. Shi, J. Liu, C. M. Li and Q. H. Yang, *Inorg. Chem.*, 2007, **46**, 7944–7952.
178. X. Shi, J. P. Li, Y. Tang and Q. H. Yang, *J. Mater. Chem.*, 2010, **20**, 6495–6504.
179. Y. Tang, Y. B. Ren and X. Shi, *Inorg. Chem.*, 2013, **52**, 1388–1397.
180. X. N. Wei and X. Shi, *J. Phys. Chem. C,* 2014, **118**, 4213–4221.
181. C. J. Reedy and B. R. Gibney, *Chem. Rev.*, 2004, **104**, 617–650.
182. M. Hartmann and D. Jung, *J. Mater. Chem.*, 2010, **20**, 844–857.
183. D. N. Tran and K. J. Balkus, *ACS Catal.*, 2011, **1**, 956–968.
184. Y. Wang, J. Xu, Y. W. Wang and H. Y. Chen, *Chem. Soc. Rev.*, 2013, **42**, 2930–2962.
185. X. Shi, J. Yang and Q. H. Yang, *Eur. J. Inorg. Chem.*, 2006, **10**, 1936–1939.
186. S. Calogero, D. Lanari, M. Orrù, O. Piermatti, F. Pizzo and L. Vaccaro, *J. Catal.*, 2011, **282**, 112–119.
187. Angeloni, O. Piermatti, F. Pizzo and L. Vaccaro, *Eur. J. Org. Chem.*, 2014, 1716–1726.
188. X. B. Ma, Y. H. Wang, W. Wang and J. Cao, *Catal. Commun.*, 2010, **11**, 401–407.
189. M. Palucki, P. J. Pospisil, W. Zhang and E. N. Jacobson, *J. Am. Chem. Soc.*, 1994, **116**, 9333.
190. B. W. Gong, X. K. Fu, J. X. Chen, Y. D. Li, X. C. Zou, X. B. Tu, P. P. Ding and L. P. Ma, *J. Catal.*, 2009, **262**, 9–17.
191. A. Hu, H. L. Ngo and W. Lin, *Angew. Chem., Int. Ed.*, 2003, **42**, 6000–6003.
192. A. Hu, H. L. Ngo and W. Lin, *J. Am. Chem. Soc.*, 2003, **125**, 11490–11491.
193. U. Costantino, F. Fringuelli, M. Nocchetti and O. Piermatti, *Appl. Catal. A*, 2007, **326**, 100–105.
194. A. Milo and R. Neumann, *Adv. Synth. Catal.*, 2010, **352**, 2159–2165.
195. A. Milo and R. Neumann, *Chem. Commun.*, 2011, **47**, 2535–2537.
196. S. Yang, L. Z. Zhao, C. Z. Yu, X. F. Zhou, J. W. Tang, P. Yuan, D. Y. Chen and D. Y. Zhao, *J. Am. Chem. Soc.*, 2006, **128**, 10460–10466.
197. B. Wang, C. Chi, W. Shan, Y. Zhang, N. Ren, W. Yang and Y. Tang, *Angew. Chem., Int. Ed.*, 2006, **45**, 2088–2090.
198. Y. Han, L. Zhao and J. Y. Ying, *Adv. Mater.*, 2007, **19**, 2454–2459.
199. S. Che, Z. Liu, T. Ohsuna, K. Sakamoto, O. Terasaki and T. Tatsumi, *Nature*, 2004, **429**, 281–284.
200. S. Y. Song, J. F. Ma, J. Yang, M. H. Cao, H. J. Zhang, H. S. Wang and K. Y. Yang, *Inorg. Chem.*, 2006, **45**, 1201–1207.
201. L. L. Gao, S. Y. Song, J. F. Ma and J. Yang, *Cryst. Growth Des.*, 2007, **7**, 895–899.
202. R. Murugavel, M. Sathiyendiran and M. G. Walawalkar, *Inorg. Chem.*, 2001, **40**, 427–434.
203. R. Pothiraja, M. Sathiyendiran, R. J. Butcher and R. Murugavel, *Inorg. Chem.*, 2004, **43**, 7585–7587.
204. F. Y. Cheng and J. Chen, *Chem. Soc. Rev.*, 2012, **41**, 2172–2192.
205. Y. P. Zhu, Y. Liu, Y. P. Liu, T. Z. Ren, T. Chen and Z. Y. Yuan, *ChemCatChem*, 2015, DOI: 10.1002/cctc.201500148.
206. Y. P. Zhu, Y. Liu, Y. P. Liu, T. Z. Ren, G. Du, T. Chen and Z. Y. Yuan, *J. Mater. Chem. A*, 2015, DOI: 10.1039/C5TA016111H.
207. H. Over, *Chem. Rev.*, 2012, **112**, 3356−3426.
208. Y. Lee, J. Suntivich, K. J. May, E. E. Perry and Y. Shao-Horn, *J. Phys. Chem. Lett.*, 2012, **3**, 399−404.
209. G. L. Tian, M. Q. Zhao, D. Yu, X. Y. Kong, J. Q. Huang, Q. Zhang, F. Wei, *Small*, 2014, **10**, 2251−2259.
210. Y. Zhao, R. Nakamura, K. Kamiya, S. Nakanishi and K. Hashimoto, *Nat. Commun.*, 2013, **4**, 2390.
211. X. Long, J. K. Li, S. Xiao, K. Y. Yan, Z. L. Wang, H. N. Chen and S. H. Yang, *Angew. Chem., Int. Ed.*, 2014, **53**, 7584−7588.
212. M. W. Kanan and D. G. Nocera, *Science*, 2008, **321**, 1072−1075.
213. D. A. Lutterman, Y. Surendranath and D. G. Nocera, *J. Am. Chem. Soc.*, 2009, **131**, 3838−3839.
214. M. W. Kanan, Y. Surendranath and D. G. Nocera, *Chem. Soc. Rev.*, 2009, **38**, 109−114.

215. Y. Surendranath, M. W. Kanan and D. G. Nocera, *J. Am. Chem. Soc.*, 2010, **132**, 16501−16509.
216. M. W. Kanan, J. Yano, Y. Surendranath, M. Dinc, V. K. Yachandra and D. G. Nocera, *J. Am. Chem. Soc.*, 2010, **132**, 13692−13701.
217. M. Risch, V. Khare, I. Zaharieva, L. Gerencser, P. Chernev, H. Dau, *J. Am. Chem. Soc*., 2009, **131**, 6936−6937.
218. A. J. Esswein, Y. S. Surendranath, S. Y. Reece and D. G. Nocera, *Energy Environ. Sci.*, 2011, **4**, 499−504.
219. H. S. Ahn and T. D. Tilley, *Adv. Funct. Mater.*, 2013, **23**, 227–233.
220. Y. Surendranath, M. Dincă and D. G. Nocera, *J. Am. Chem. Soc.*, 2009, **131**, 2615–2620.
221. G. Alberti, M. Casciola, F. Marmottini and R. Vivani, *J. Porous Mater.*, 1999, **6**, 299–305.
222. Z. Y. Yuan, T. Z. Ren, A. Azioune, J. J. Pireaux and B. L. Su, *Catal. Today*, 2005, **105**, 647–654.
223. S. K. Das, M. K. Bhunia, A. K. Sinha and A. Bhaumik, *ACS Catal.*, 2011, **1**, 493–501.
224. A. Clearfield, *J. Mol. Catal.*, 1984, **27**, 251–162.
225. I. C. Marcua, I. Sandulescu and J. M. M. Millet, *Appl. Catal. A*, 2002, 27, 309–320.
226. Y. P. Bi, H. Y. Hu, S. X. Ouyang, G. X. Lu, J. Y. Cao and J. H. Ye, *Chem. Commun.*, 2012, **48**, 3748–3750.
227. G. Wang, B. Huang, X. Ma, Z. Wang, X. Qin, X. Zhang, Y. Dai and M. H. Whangbo, *Angew. Chem., Int. Ed.*, 2013, **52**, 1–5.
228. M. Chen, L. L. Shao, H. B. Yang, Q. Y. Zhao and Z. Y. Yuan, *Electrochimica Acta*, 2015, **168**, 59–68.
229. M. Chen, L. L. Shao, H. B. Yang, T. Z. Ren, G. Du and Z. Y. Yuan, *Electrochimica Acta*, 2015, **167**, 278–286.
230. A. Morozan and F. Jaouen, *Energy Environ. Sci.*, 2012, **5**, 9269–9290.
231. J. K. Sun and Q. Xu, *Energy Environ. Sci.*, 2014, **7**, 2071–2100.
232. X. Z. Lin and Z. Y. Yuan, *RSC Adv.*, 2014, **4**, 32443–32450.
233. T. Z. Ren, Z. Y. Yuan, A. Azioune, J. J. Pireaux and B. L. Su, *Langmuir*, 2006, **22**, 3886–3894.
234. G. L. Zhao, X. J. Zhang, T. H. Chen and Z. Y. Yuan, *Mater. Sci. Eng. B*, 2006, **131**, 263–266.
235. Y. L. Liu, Y. P. Zhu, M. Li and Z. Y. Yuan, *Acta Chimica Sinica*, 2014, **72**, 521–536.
236. T. Y. Ma, L. Liu and Z. Y. Yuan, *Chem. Soc. Rev.*, 2013, **42**, 3977–4003.

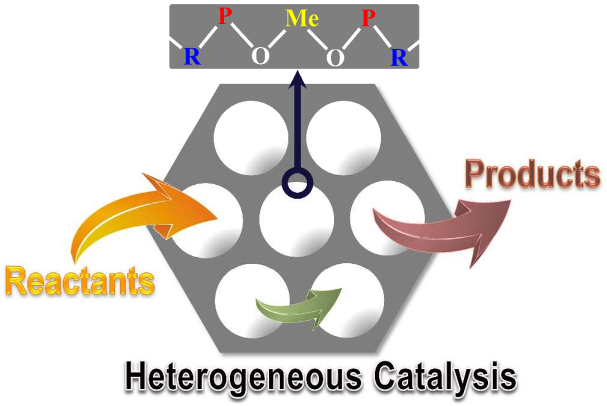

Meosporous metal phosphonates have received increasing attention as promising heterogeneous catalysts due to the abundant framework compositions and controllable porosity.